DENTAL MATERIALS 35 (2019) 1173–1193

Available online at www.sciencedirect.com

ScienceDirect

journal homepage: www.intl.elsevierhealth.com/journals/dema

Effect of the degree of conversion of resin-based composites on cytotoxicity, cell attachment, and gene expression

Masako Fujioka-Kobayashi[a,1], *Richard J. Miron*[b,1], *Adrian Lussi*[c], *Reinhard Gruber*[d], *Nicoleta Ilie*[e], *Richard Bengt Price*[f,1], *Gottfried Schmalz*[b,g,*,1]

[a] *Department of Cranio–Maxillofacial Surgery, Inselspital, Bern University Hospital, University of Bern, Freiburgstrasse, Bern, 3010, Switzerland*
[b] *Department of Periodontology, School of Dental Medicine, University of Bern, Freiburgstrasse 7, Bern, 3010, Switzerland*
[c] *Department of Preventive, Restorative and Pediatric Dentistry, School of Dental Medicine, University of Bern, Freiburgstrasse 7, Bern, 3010, Switzerland*
[d] *Department of Oral Biology, Dental School, Medical University of Vienna, Sensengasse 2a, Vienna, 1090, Austria*
[e] *Department of Conservative Dentistry and Periodontology, University Hospital, LMU Munich, Goethestr 70, Munich, 80336, Germany*
[f] *Department of Dental Clinical Sciences, Faculty of Dentistry, Dalhousie University, 5981 University Ave., Halifax, Nova Scotia, B3H 4R2, Canada*
[g] *Department of Conservative Dentistry and Periodontology, University Hospital Regensburg, University of Regensburg, Regensburg, 93042, Germany*

ARTICLE INFO

Article history:
Received 12 April 2019
Accepted 14 May 2019

Keywords:
Resin-based composites
Light curing unit
Resin conversion
Cytotoxicity

ABSTRACT

Objective. This study investigated the influence of the degree of conversion (DC), resin-based composites (RBC) composition, and the effect of additional violet light from one light curing unit (LCU) on cell attachment/growth, eluate cytotoxicity, and gene expression.
Methods. The effect of different DC of RBCs on human gingival fibroblasts (HGFs) when cultured directly onto cured RBCs, and when exposed afterwards to eluates in cell culture medium was examined. Venus® (RBC-V; Bis-GMA-based) and Venus Pearl® (RBC-P; TCD-DI-HEA and UDMA-based) were cured using a single emission peak (blue) light, Translux Wave®; TW and a dual emission peak (blue-violet) light, Translux 2 Wave®; T2W. To determine the value of the additional violet light from the T2W, exposure times and distances were adjusted to deliver similar radiant exposures (RE) from the blue region of both lights at five different RE levels from 1.5 J/cm^2 to 28.9 J/cm^2.

* *Corresponding author at*: Department for Conservative Dentistry and Periodontology, University Hospital Regensburg, Regensburg, D-93042, Germany.
E-mail address: Gottfried.Schmalz@klinik.uni-regensburg.de (G. Schmalz).
https://doi.org/10.1016/j.dental.2019.05.015

Results. Both RBCs light-cured with the T2W at higher REs resulted in higher DC, increased cell adhesion and decreased eluate cytotoxicity. RBC-V induced greater cell adhesion, lower mRNA levels of pro-inflammatory markers, and higher mRNA levels of a proliferation marker than RBC-P. Wettability was the same for both RBCs. Toxicity decreased with increasing number of elution cycles. The initial eluates from RBC-P had a lower toxicity than from RBC-V.

Significance. RBCs cured with T2W (delivering both blue and violet light) at higher RE had greater DCs. The greatest DC and the least cell reactions were observed when the RE was >25 J/cm^2.

1. Introduction

Resin-based composite (RBC) restorations are routinely used in dental practice [1,2], and their use will continue to rise with the global phase down in the use of amalgam as part of the Minamata Convention on Mercury [3]. The clinical success of these restorations requires that the RBCs achieve sufficient mechanical properties and exhibit good biocompatibility in the oral cavity. Despite their widespread use, delivering a successful RBC in deep proximal cavities continues to be a challenge, partly because the RBC at the bottom of the approximal cavity floor is often 7 mm or more away from the tip of the light curing unit (LCU), and this region is often difficult to access with the curing light. Also, as the thickness increases, there is a logarithmic decrease in the light transmission through both the RBC and the tooth, further reducing the amount of light that reaches the bottom of the restoration [4]. Thus, the RBC at the bottom of the proximal box is often less well polymerized than the top surface of the RBC.

RBCs are complex mixtures of inorganic filler particles, matrix resins, coupling agents and additives. The extent to which the monomers are converted to a polymer, the degree of conversion (DC) of the functional groups of the RBC, has been reported to range from 35 to 77% [5]. In the mouth, the RBCs will release some of their unreacted monomer content and other substances [5,6] and it is estimated that approximately 2 wt.% of the organic matrix; e.g., Bis-GMA (0.4 wt.%–1.5 wt.%), TEGDMA (0.04–2.3 wt.%), is elutable from the tested RBC in aqueous media [7–9]. The amount of elutable substances affects the biocompatibility of the RBCs for it is known that some monomers or compounds eluted from composites may cause both local and systemic adverse reactions [10]. The greatest release of these elutable substances (e.g., HEMA, TEGDMA, Bis-GMA, UDMA) takes place within the first few hours after photo-curing, and it declines asymptotically over time if the incubation solution is not refreshed [10,11]. However, even after 90 and 180 days, refreshed solutions still contain elution products (e.g., TEGDMA, Bis-GMA, Bis-EMA, BPA) from several brands of RBC [12].

The DC of RBCs affects the release of potentially toxic substances that are present within the RBC [13]. Inadequate polymerization of the RBCs has been shown to result in increased solubility and water sorption due to the reduced conversion of the monomers [14]. One factor that influences the DC of light cured RBCs is the radiant exposure (RE; dose or amount of energy delivered per unit area) and the wavelengths of light that are delivered to the RBC. Accordingly, the cytotoxicity of RBCs and their respective dental adhesives has been reported to be dependent upon the LCU; [15,16] a high power quartz-tungsten halogen LCU that was claimed to deliver an irradiance of 3000 mW/cm^2 produced a significantly higher cell viability of some RBCs compared to when a quartz-tungsten-halogen LCU that was claimed to deliver an irradiance of 600 mW/cm^2 was used. However, in other studies, no difference in the DC and cytotoxicity of dental adhesives were found when the distance between light tip and material was increased up to 7 mm [17]. No systematic studies on the effect of DC and emission spectrum from the LCU on cytotoxicity of RBCs are available. Such studies are necessary because the DC depends more on the RE, and the emission spectrum from the LCU and less upon the irradiance value alone. Since a high irradiance delivered at the wrong wavelength will not cure the resin, an appropriate combination of wavelengths from the LCUs that match the absorption characteristics of the photoinitiators is required to achieve a satisfactory DC. This was not an issue when using quartz-tungsten halogen LCUs that emit a broad spectrum of filtered light from 380 to 515 nm. However, due to the nature of the light emitting diode (LED) emitter, LED-curing lights do not produce such a broad emission spectrum unless they include multiple different LED emitters to provide multiple emission peaks to cover between 380–515 nm. This is unlike the single emission peak LCUs that emit just a single emission peak that is usually between 450 and 475 nm [6]. The manufacturers of these multiple peak wavelength LCUs claim that these broad-spectrum LEDs cure all RBCs containing a variety of photoinitiators, such as 2,4,6-trimethylbenzoyldiphenylphosphine oxide (Lucirin TPO) or phenylpropanedione (PPD), whose absorption peak is close to 390 nm, as well as camphorquinone (CQ), whose peak absorbance is close to 470 nm [6,18].

When the RBC is placed into sub-gingival regions, it interacts with epithelial cells and fibroblasts from gingival tissues. In general, a good attachment of these cells to biomaterials is desired to support cell spreading, proliferation and new tissue formation [19,20]. The adhesive behavior of osteoblasts or fibroblasts to model surfaces is dependent upon

[1] These authors contributed equally to this work.

the chemistry of these surfaces [20,21]. Schweikl et al. used self-assembled monolayers that were terminated by various functional chemical groups to demonstrate that cell proliferation on hydrophobic surfaces, such as *n*-octyltriethoxysilane, can be as high as the cell proliferation that occurs on moderately hydrophobic surfaces and hydrophilic oxidized surfaces [20]. Moreover, the cells attached to biomaterials showed different gene expression patterns. It was reported that human osteoblasts cultured on titanium or zirconia expressed mRNAs differently for specific markers including Runx-2, -3, BMP-7, alkaline phosphatase, osteopontin, osteocalcin, osteonectin, Type I collagen, bone sialoprotein and integrin β3, primarily due to small differences in the roughness and marginally due to the material composition in the initial phase of attachment and proliferation [22,23]. Although several studies have investigated the effect of the RBC on cell behavior by testing eluates from RBCs [10,24–27], the direct interaction between cells and RBC surfaces, especially the gene expression of cells on RBCs, requires further study.

The present study examines the DC, the wettability, cell attachment, cytotoxicity of eluates, and gene expression after cells were exposed to two different RBCs after they had been photocured with either a single emission peak or a multiple emission peak LED LCU. To determine the effect of the violet light, a similar amount of blue light was delivered from both LCUs, and the additional light and RE was provided by the violet LED emitter from one LCU. Human gingival fibroblasts (HGFs) were cultured (1) directly on the cured RBC materials to evaluate the direct contact interaction between cells and the materials and (2) in eluates from the materials to assess the effects of the eluted substances on cell behavior. The null hypotheses were that the DC, RBC composition, and the additional violet light from one LCU would not influence cellular attachment/growth, eluate cytotoxicity, or gene expression.

2. Materials and methods

2.1. *Preparation of test specimens*

Two commercial RBCs from the same manufacturer; Venus shade A3® (RBC-V, a submicron hybrid RBC) and Venus Pearl shade A3® (RBC-P, a nano hybrid RBC) were studied (Table 1). The uncured RBCs were filled into white semi-opaque Teflon rings that had a 5 mm inner diameter and were 2 mm deep. The filled rings were placed on a glass plate, and the top and bottom RBC surfaces covered with a Mylar strip (Patterson, Montreal, Quebec, Canada). The light exposure conditions are provided in Table 2. Based on the fact that the manufacturer recommends a 20 s exposure time for each 2 mm increment of material, five different REs were used to irradiate the specimens. These different REs were achieved by adjusting the distance between the light tip and the specimen (0, 4 or 12 mm) and by adjusting the exposure time (5, 10 or 20 s). To avoid any material changes, the specimens were produced under clean conditions and the operator used gloves and wore a face mask. The specimens were not sterilized or cleaned with any chemicals, and cell culture experiments did not show any bacterial contamination of these specimens. Every effort was made to deliver similar REs of blue-light from both LCUs;

Table 1 – Material specifications (information supplied by Kulzer GmbH).

Composite, shade	Lot #	Composition
Venus A3® (RBC-V)	010036A	BIS-GMA matrix, 58,7 % filler by volume, which is Barium Aluminium Fluoride glass (⌀ 0.7 μm; max. < 2 μm) • Highly dispersive Silicon Dioxide (⌀ 0.04 μm); photoinitiator system: camphorquinone (CQ) / amine
Venus Pearl A3® (RBC-P)	010504A	TCD-DI-HEA and UDMA, approximately 59% filler by volume, with 58% organic filler by volume and a particle size of 5 nm – 5 μm • Barium Aluminium Fluoride glass • Pre-polymerized filler • Highly discrete nanoparticles; photoinitiator system: camphorquinone (CQ) / amine and Lucirin (2,4,6-Trimethylbenzoyl-diphenyl-phosphinoxid; TPO), phenyl-propanedione (PPD)

a single (blue) emission peak (Translux Wave®; TW, Kulzer GmbH, Hanau, Germany) and a dual (violet–blue) emission peak LED (Translux 2 Wave®; T2W, Kulzer GmbH). Thus, the additional RE from the T2W could be attributed to the violet light from this LCU. After they had been made, the specimens were immediately placed into sterile bags and dark stored at room temperature.

Additional specimens were prepared by Kulzer GmbH: (1) RBC-V and RBC-P with the surface layer removed and polished (surface treated specimens); (2) RBC-V and RBC-P without surface treatment; and (3) RBC-V and RBC-P without filler particles (matrix polymer with initiator system only). These specimens were light cured for 20 s and a distance of 4 mm using the T2W. The surface treated specimens were ground with a polishing machine (TegraPol-35, Struers, Ballerup, Denmark). In the first step, approximately 50 μm were removed using silicon carbide (P1000/Grit 500). Polishing was then performed using silicon carbide (P4000) at 180 rpm. Both grinding and polishing were performed using ample water cooling.

2.2. *Characterization of LCU*

The spectral radiant powers from the two fully charged LCUs were examined in the 350–550 nm wavelength range of the spectrum to determine the REs delivered to the specimens in the blue wavelength range (>420 nm). To measure the power delivered by the LCUs to the 5 mm diameter specimens, the LCUs were fixed in front of a restricted 4 mm aperture into a 6-inch diameter integrating sphere (Labsphere, North Sutton, NH, USA) connected to a fiber-optic spectroradiometer (USB 4000, Ocean Optics, Dunedin, Fla, USA). A 50 μm thick Mylar Strip (Patterson) was placed over this 4 mm aperture to replicate the experimental conditions where the Mylar strip covered the RBC specimen. An internal light source within the sphere (Labsphere) that was traceable to a National Institute of Standards and Technology (Gaithersburg, MD, USA) reference was used to calibrate the system before measuring the LCUs. The lights and exposure conditions were measured in

Table 2 – Light exposure conditions.

Materials	LCU	Time	% of maximum RE	Denomination
Venus A3® (RBC-V)	Translux Wave (TW)	5 sec	6.25%	V-TW-1
		10 sec	12.5%	V-TW-2
		20 sec	25%	V-TW-3
		20 sec	50%	V-TW-4
		20 sec	100%	V-TW-5
	Translux 2 Wave (T2W)	5 sec	6.25%	V-T2W-1
		10 sec	12.5%	V-T2W-2
		20 sec	25%	V-T2W-3
		20 sec	50%	V-T2W-4
		20 sec	100%	V-T2W-5
Venus Pearl A3® (RBC-P)	Translux Wave (TW)	5 sec	6.25%	P-TW-1
		10 sec	12.5%	P-TW-2
		20 sec	25%	P-TW-3
		20 sec	50%	P-TW-4
		20 sec	100%	P-TW-5
	Translux 2 Wave (T2W)	5 sec	6.25%	P-T2W-1
		10 sec	12.5%	P-T2W-2
		20 sec	25%	P-T2W-3
		20 sec	50%	P-T2W-4
		20 sec	100%	P-T2W-5

triplicate with the LCUs being removed and replaced in front of the sphere for each measurement.

2.3. *Degree of conversion (DC)*

The degree of conversion (DC) was measured using Fourier Transform mid-infrared Spectroscopy (Vertex 70, Bruker, Billerica, MA, USA). This spectrometer was equipped with a temperature controlled Attenuated Total Reflectance (ATR) unit (Golden Gate, Specac, Orpington, Kent, UK) containing a single reflection monolithic 2.0 mm × 2.0 mm diamond prism. The focus point at the center of the 2 mm × 2 mm square diamond crystal is approximately 1 mm in diameter and the depth of penetration of light into the RBC sample on the ATR crystal is approximately 2 microns (Specac). The DC of three replicates of each group was measured at the bottom center of the specimens. The mid-IR spectrometer data collection started at a rate of 8 measurements per second at a resolution of 4 wavenumbers. After 10 s, the LCU was switched on, and after the DC at the bottom had been recorded for 180 s, a static measurement of the DC was recorded from an average of 20 scans. To calculate the DC, a baseline correction (concave rubberband) with 5 iterations was performed using the Opus v 7.8 software (Bruker, Billerica, MA, USA). The decrease of the integrated area of an aliphatic C=C peak at 1638 cm^{-1} to an internal reference aromatic C=C peak at 1608 cm^{-1} was used to calculate the DC for RBC-V. RBC-P did not exhibit an aromatic peak at 1608 cm^{-1} that could be used as an internal standard. Consequently, the carbon—carbon double bond conversion was calculated from the ratio of the areas of the aliphatic —C=C— band between 1643–1630 cm^{-1} wavenumbers in the polymerized compared to the unpolymerized RBC.

2.4. *Wettability measurements*

The wettability was measured on two specimens each for (1) RBC-V cured with T2W for 20 s from a 4-mm distance and (2) RBC-P cured with T2W for 20 s from a 4 mm distance (V-T2W-4 and P-T2W-4). The measurements were performed in triplicate on both sides of each specimen before and after incubation in a cell culture medium that consisted of DMEM (Gibco Life Technologies, Carlsbad, CA, USA), 10% fetal bovine serum (FBS; Gibco) and 1% antibiotics (Gibco). Each specimen was placed in 600 μl of cell culture medium for 24 h at 37 °C without CO_2. The contact angles were measured by the drop shape analysis system (DAS 10-MK2; Krüss, Hamburg, Germany) using a sessile droplet at room temperature. In summary, a 5 μl water droplet from a 0.5 mm diameter tube was placed on each specimen, and the contact angle was measured using an automatic baseline and circle fitting. The means of the left and right contact angles were calculated and used.

2.5. *Eluate preparation*

Eluates of RBC specimens were prepared following the recommendations of ISO 10993-12 using a ratio of 117.8 mm^2 sample surface area/ml cell culture medium [28]. Ten cured RBC specimens taken out from the Teflon rings were placed in 6 ml cell culture medium consisting of DMEM (Gibco Life technologies, Carlsbad, CA, USA (Gibco)), 10% fetal bovine serum (FBS; Gibco) and 1% antibiotics (Gibco) in a 25 ml tube and eluted at 37 °C in a shaking incubator at 60 rpm (Kuhner AG, Basel, Switzerland). Eluates were collected every 24 h for 10 days (Fig. 1). 6 ml of culture medium per tube were collected, frozen at −20 °C before cell testing and replaced with 6 ml of additional fresh culture medium. The 1st, 2nd, 3rd and 10th eluates were used for the experiments. Control media stored for the same time periods were used as control eluate samples at each time point.

2.6. *Cell culture*

Primary human gingival tissues were harvested from healthy donors undergoing third molar extractions, and morphologically spindle-shaped HGFs were cultured as described in previous studies [29,30] after approval of the Ethical Committee of the Medical University of Vienna (EK Nr. 631/2007).

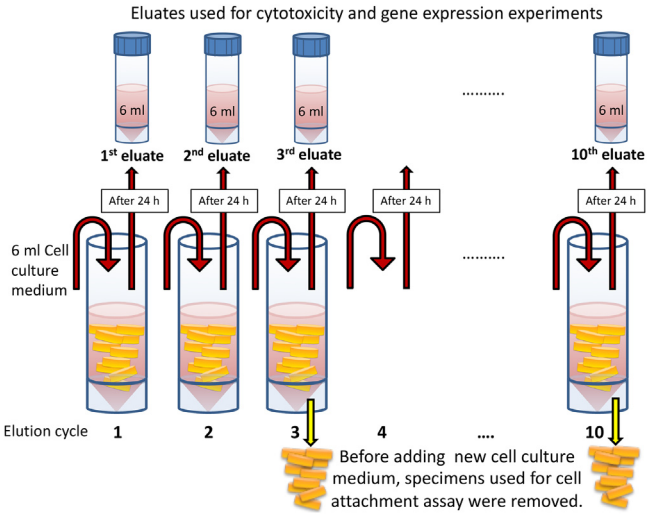

Fig. 1 – Schematic showing how the RBC specimens and eluates were used in the experiments.

Cells were cultured in a humidified atmosphere at 37 °C in cell growth medium (DMEM, 10% fetal bovine serum (FBS) and 1% antibiotics) and detached from tissue culture plastic using 0.25% EDTA-Trypsin (Gibco) before reaching confluency. The cells used for experimental seeding were from passages 4 to 6.

2.7. *Cell attachment on RBCs*

To determine the cell attachment, nine specimens from each of the 20 groups of RBCs cured under the condition shown in Table 2, were exposed three or ten times to cell culture medium with no cells (Fig. 1). Then, cells were seeded onto the RBC discs at a density of 10,000 cells per well in 96-well plates. After 24 h of incubation in a humid atmosphere of 5% CO_2 at 37 °C, the cells were fixed with 4% formaldehyde for 2 min. Then cells were permeabilized by methanol for 20 min and stained with Giemsa solution (MERCK, Darmstadt, Germany) for 15 min. After rinsing in sterile water and drying, the specimens were examined under a microscope (Olympus SZX7, Tokyo, Japan) and the numbers of cells on the RBCs were counted. One image per sample was taken at 5.6× magnification from the middle portion of the sample. Cells were distinguished by their shape as either round or spread cells and counted manually by using the counting tool in Photoshop CS5.1 software (Adobe, San Jose, CA, USA).

The additional groups of RBCs (1) RBC-V and RBC-P with surface treatment, (2) RBC-V and RBC-P without surface treatment, and (3) RBC-V and RBC-P without filler particles were further tested after the 10th elution, and cell attachment was recorded after 24 h of incubation.

Cell attachment on either the top or bottom of the RBCs was compared in three groups; of V-T2W-1, V-T2W-4, and V-T2W-5 (see Table 2) and specimens were prepared and marked with a scratch on the top surface of the composite. 10 specimens per test group were used just after the 3rd eluate collection. Cells were seeded on either the top or bottom surface of the composite discs at a density of 10,000 cells per well in 96-well plates. After 24 h of incubation, a cell attachment assay was performed as described above.

2.8. *Cell viability assay with RBC eluates*

HGFs were seeded in 96-well plates at a density of 5,000 cells per well. One day after cell seeding, the media were replaced by eluates collected at each time point. Cell viability was quantified, using 3-(4,5-Dimethylthiazol-2-yl)-5(3-carboxyme-thonyphenol)-2-(4-sulfophenyl)-2H-tetrazolium, inner salt (MTS) assay (Promega, Madison, WI, USA). This is a colorimetric method to determine the number of viable cells based on the principle that mitochondria in viable cells reduce MTS to a water-soluble coloured formazan product. The intensity was quantified using an ELx808 Absorbance Reader (BIO-TEK, Winooski, VT, USA) after 24 h incubation/exposure to the eluates. Optical density readings were converted into percent relative cell viability setting the control cultures (that contained no toxicant) as 100%.

2.9. *Real-time PCR analysis*

PCR analyses were performed on cells which had been grown on test materials and cells exposed to eluates from test materials. For experiments using cells grown on test materials, cells were seeded at a density of 10,000 cells on the materials after the 3rd elution cycle in 96 well culture plates. For experiments using eluates, 50,000 cells per well in 24 well dishes were grown for 24 h and then were exposed to the 3rd eluates. Total RNA was isolated using High Pure RNA Isolation Kit (Roche, Basel, Switzerland) according to the manufacturer's instruction either at 3 days post cell seeding on RBCs or 3 days post 3rd eluate stimulation. A Nanodrop 2000c (Thermo, Wilmington, DE, USA) was used to quantify total RNA levels. Real-time RT-PCR was performed using a Roche Master mix and quantified on an Applied Biosystems 7500 Real-Time PCR Machine. Primer sequences for genes encoding interleukin-1, -6, -8 and -11 (IL-1, IL-6, IL-8 and IL-11), tumor necrosis factor-α (TNF-α), integrin β3, ki-67, Transforming growth factor β (TGF-β), platelet-derived growth factor (PDGF), adrenomedullin (ADM), caspase 3, 8 and 9, annexin A5, and β-actin were fabricated with primer sequences according to Table 3. The ΔΔCt method (a comparative CT method) was used to calculate gene expression levels normalized to the expression of the housekeeping gene β-actin.

2.10. *Protein release quantification (ELISA)*

To determine the quantity of cytokine release from HGFs after exposure to RBCs or RBC eluates, ELISA quantification assays were utilized. For experiments using cells grown on test RBCs, cells were seeded at a density of 10,000 cells on the materials after the 3rd elution cycle in 96 well culture plates. For experiments using eluates, cells were cultured at a density of 50,000 cells per well in 24 well dishes and exposed to 3rd eluates. The supernatants were collected after 3 days incubation for both experiments of culture on RBC and in RBC eluates. IL-6 (DY206-05, range = 9.38–600 pg/mL), TGF-β (DY240, range = 31.20–2000 pg/ml) and VEGF (DY293B-05, range = 31.20–2000 pg/mL) were quantified using an ELISA

Table 3 – List of primer sequences for real-time PCR analysis.

Gene	Forward primer	Reverse primer
hIL-1	ggttgagtttaagccaatcca	ggtgatgacctaggcttgatg
hIL-6	gaaaggagacatgtaacaagagt	gattttcaccaggcaagtct
hIL-8	atgacttccaagctggccgt	tccttggcaaaactgcacct
hTNF-α	cagcctcttctccttcctgat	gccagagggctgattagaga
hIntegrin β3	gtgctgacgctaactgacc	catggtagtggaggcagagt
hKi-67	gaggtgtgcagaaaatccaaa	ctgtccctatgacttctggttgt
hTGF-β	actactacgccaaggaggtcac	tgcttgaacttgtcatagatttcg
hPDGF	cacacctcctcgctgtagtattta	gttatcggtgtaaatgtcatccaa
hADM	ggacatgaagggtgcctctc	tgttcatgctctggcggtag
hIL-11	tgcacctgacacttgactgg	agtcttcagcagcagcagtc
hCaspase 3	ttcagaggggatcgttgtagaagtc	caagcttgtcggcatactgtttcag
hCaspase 8	ctgctggggatggccactgtg	tcgcctcgaggacatcgctctc
hCaspase 9	atggacgaagcggatcggcggctcc	gcaccactgggggtaaggttttctag
hAnnexin A5	cagtctaggtgcagctgccg	ggtgaagcaggaccagactgt
hβ-actin	ccaaccgcgagaagatga	ccagaggcgtacagggatag

kit (DuoSet, R&D Systems, Minneapolis, MN, USA) according to the manufacturer's protocol. Absorbance was measured at 450 nm and 570 nm using an ELx808 Absorbance Reader, and OD values at 570 nm were subtracted from the readings at 450 nm ($OD_{450} - OD_{570}$). Each protein concentration was calculated from the standard carve.

2.11. *Statistical analysis*

To characterize the LCUs, three separate measurements were made of the spectral radiant power and the radiant power emitted between 350 nm and 550 nm and the mean values with the standard deviation (SD) are reported (Table 4).

To determine the DC for the RBCs made using the different radiant exposures, three independent specimens were tested per group. The DC data for each composite was analyzed separately using a two-way ANOVA on the raw data and the normalized data using the Box-Cox transformation. Mean DC results with SD are reported in Table 5.

To determine the wettability, six independent measurements were performed. The medians with 25/75 percentiles are reported, and statistical evaluation was performed using a non-parametric Kruskal–Wallis test and Wilcoxon matched-pairs rank test at $p < 0.05$.

For cell attachment assay on RBCs, nine independent specimens were assessed. Cell proliferation assays testing eluates were repeated 3 times in triplicate. Experiments for real-time PCR and protein release assays were repeated 3 times in duplicate. Medians and interquartile ranges are reported in 5–7,10–12 and 15. For the real time PCR medians of the three independent experiment are reported (8, 10, 13, 14). The values were analyzed for statistical significance using the non-parametric Kruskal–Wallis test for cell proliferation assay, gene expression analysis, and protein release assay using GraphPad Prism 6.0 software (GraphPad Software, Inc., La Jolla, CA, USA). For all statistical tests, the significance level of p values was set to <0.05. Correlation analyses relating DC to REs or cell reaction to DC were performed using the original data, and each regression curve was calculated using GraphPad Prism 6.0 software.

3. Results

3.1. *Characterization of the LCUs*

Representative emission spectra from the two LCUs are shown in Fig. 2. They clearly show the single emission peak for TW in the blue wavelength area and the two peaks for the T2W with the additional peak in the violet wavelength region. However, by adjusting the distance from the target, the peaks in the blue region above 420 nm became similar for both LCUs.

As shown in Table 4, the REs (J/cm^2) delivered to the specimens ranged from 1.5 J/cm^2 from the TW and 1.7 J/cm^2 from the T2W to 24.5 J/cm^2 from TW and 28.9. J/cm^2 from the T2W. The peak wavelength in the blue spectrum from both lights was almost identical (see above) with only differences in the violet wavelength range. Although both lights delivered the same power and RE in the blue range (>420 nm), when the violet light was included, the maximum RE delivered to the specimens increased to 28.9 J/cm^2 from the T2W. Thus, approximately 15% of the light from the T2W is from the violet LED, and this is the reason why the RE is greater from the T2W compared to TW.

3.2. *Degree of conversion (DC)*

The results for the degree of conversion (DC) are reported in Table 5 and Fig. 3. Both materials (RBC-V and RBC-P) demonstrated a logarithmic relationship (R^2 ranging from 0.944 to 0.973) between the RE and the DC achieved (Fig. 3). The measured DC of the RBC-P was generally lower compared to RBC-V. A plateau for DC was reached after a RE of about 15 J/cm^2, except for the combination of RBC-P and TW (about 25 J/cm^2). The results for the raw and the normalized data agreed. Both factors (LCU and RE) and their interaction were significant ($p < 0.001$).

Using T2W matching the RE in the blue wavelength range to TW exposed for 10 s and using the 25% level as the reference, in both cases, and for both RBCs, as the RE increased, the DC increased, but the increase in DC was the greatest between the two lowest REs.

For RBC-V, the T2W always produced the greatest DC values ($p = 0.007$). For RBC-P, the T2W produced the greatest DC values

Table 4 – Light exposure conditions and radiant exposure (RE) for the test specimens; wavelength range 350–550 nm; radiant exposure for T2W refers to the radiant exposure of the combined emissions in the blue and the violet regions (means ± SD, n = 3). The additional radiant exposure comes from the violet range of the T2W.

LCU	% Power	Irradiance (mW/cm^2 ± SD)	Radiant exposure (RE) (J/cm^2 ± SD)		
			Time 5 (sec)	Time 10 (sec)	Time 20 (sec)
TW (350–550 nm)	100	1227 ± 20			24.5 ± 0.4
	50	622 ± 28			12.4 ± 0.6
	25	309 ± 6	1.5 ± 0.1	3.1 ± 0.1	6.2 ± 0.1
T2W Matching the Blue Spectrum to the TW	100	1143 ± 23			28.9 ± 0.5
	50	639 ± 18			13.9 ± 0.4
	25	344 ± 31	1.7 ± 0.2	3.4 ± 0.3	6.9 ± 0.6

Table 5 – Radiant exposures, REs and % degree of conversion, DC (means and SD, n = 3).

Materials	LCU	Radiant exposure (J/cm^2)	DC (%)	SD
RBC-V	TW	1.5	25.2	2.1
		3.1	40.4	1.9
		6.2	45.4	1.6
		12.4	47.6	1.9
		24.5	50.3	1.7
	T2W - Matching the RE in the blue range with the additional energy coming from the violet range	1.7	25.6	2.2
		3.4	41.3	2.3
		6.9	46.3	0.8
		13.9	49.4	0.8
		28.9	51.9	0.7
RBC-P	TW	1.5	0.7	1
		3.1	27.8	1.8
		6.2	36	3.4
		12.4	40.6	2.6
		24.5	48.8	1
	T2W - Matching the RE in the blue range with the additional energy coming from the violet range	1.7	0.7	1
		3.4	30.1	2.5
		6.9	39.2	1.7
		13.9	44.9	2.1
		28.9	48.2	1.7

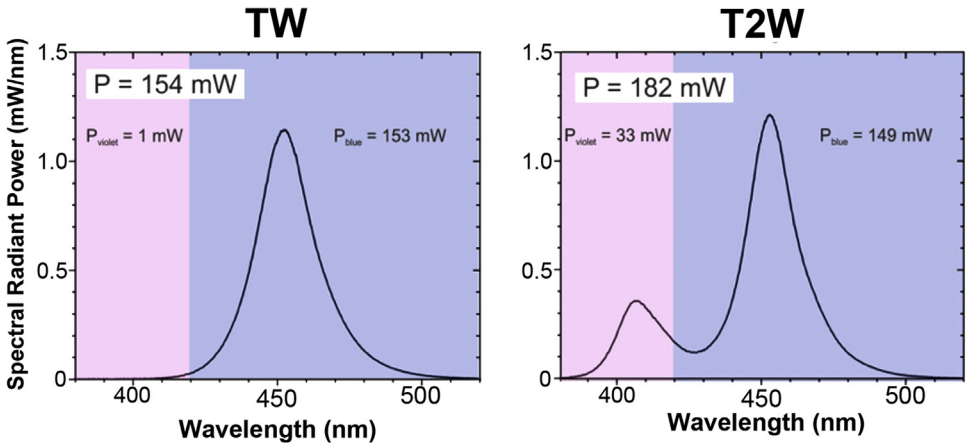

Fig. 2 – Radiant power delivered to the specimens from the Translux Wave (TW) and Translux 2 Wave (T2W); both LCUs delivered similar powers (P_{blue}) above 420 nm, but the T2W delivered additional power (P_{violet}) below 420 nm.

(p = 0.0001) in all cases except for at the highest RE level where they were not significantly different (p = 0.139).

3.3. *Wettability*

Before elution in the cell culture medium, contact angles for both RBC-V and RBC-P cured under the same conditions (T2W-4) ranged between 68.4° and 81.5° for RBC-V and between 67.4° and 90.4° for RBC-P. After 24-h incubation in the cell culture medium, the contact angles on both, RBC-V and RBC-P, significantly decreased when compared to initial values (Fig. 4). However, there were no significant differences in wettability between the two RBCs (V-T2W-4 and P-T2W-4).

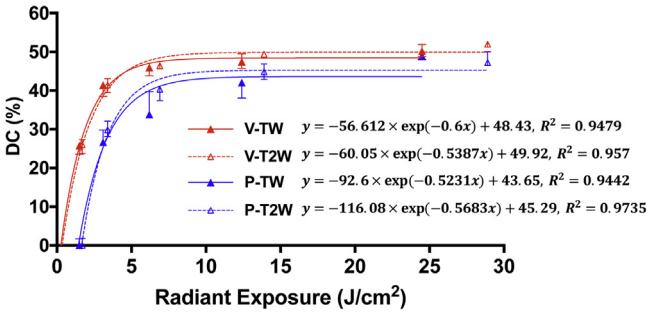

Fig. 3 – Degree of Conversion (DC) on RBC-V and RBC-P related to the radiant exposure RE delivered by the TW and T2W LCUs. The graph represents the medians with 25/75 percentiles and fitting curves (one-phase association line, least squares fit).

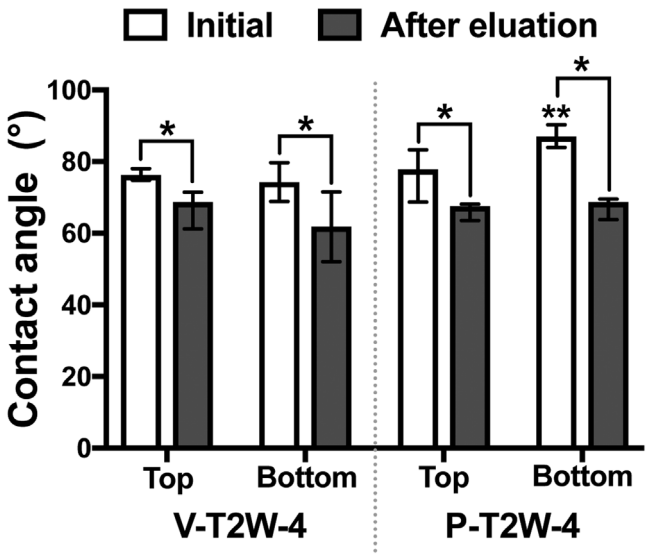

Fig. 4 – Changes of contact angles of the top and bottom surfaces of composites before and after elution in cell culture medium for 24 h. (* denotes a significant difference between groups, $p < 0.05$, ** denotes significantly higher than all other initial specimens before elution, $p < 0.05$, $n = 6$ medians with 25/75 percentiles).

3.4. *Cell attachment and growth on RBCs*

Preliminary experiments showed that cell growth on the composite surface (data not shown) did not occur on specimens until after one or two elution cycles in cell-free culture medium. Therefore, the tests were performed on the RBCs after three and ten elutions in the cell culture medium. The surfaces of the two sides of the specimens were compared for cell attachment and growth to assess the effect of sample thickness (Fig. 5, Supp. Fig. 1). These tests were performed on RBC-V after the 3 elution cycles of the specimens cured with 3 different REs (1.7, 13.9 and 28.9 J/cm^2) from the T2W LCU. There was no significant difference for cell attachment between the top and bottom of specimens in all groups (Fig. 5, Supp. Fig. 1). These data suggest that the 2 mm thickness of specimens

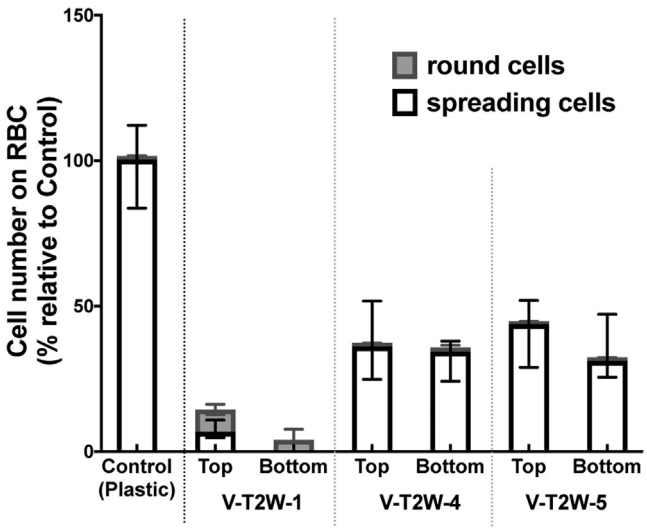

Fig. 5 – Relative cell attachment after 24 h when seeded either on the top or bottom surface of 3 different composites (V-T2W-1, V-T2W-4, and V-T2W-5) after 3 elution cycles. Both the numbers of round cells and spreading cells attached to the specimens were calculated. No significant differences were observed between the top and bottom of the specimens. (100% = optimal density reading of control cultures. $p < 0.05$. $n = 9$ medians with 25/75 percentiles).

cured from one side (top) did not result in a significantly different cell growth rate between the top and the bottom on the RBC specimens for the whole range of REs used in this study. Therefore, the cell attachment and growth were compared for all 20 groups of RBCs without the distinction of the sides (top and bottom) of specimens after 3 and 10 elution cycles in the cell culture medium.

Fig. 6 shows that RBC-V specimens generally had higher cell numbers when compared to RBC-P and cells showed a rounder morphology (indicating some alteration) on RBC-P, but less or none was observed on samples of RBC-V. This was observed for the majority of specimens both after 3 and 10 elution cycles. Cell attachment was consistently improved for the 10th elution when compared to the 3rd elution, which was statistically significant for REs of 6.9 and 13.9 J/cm^2 for V-T2W, >6.2 J/cm^2 for V-TW, >6.9 J/cm^2 for P-T2W, and >12.4 J/cm^2 for P-TW. Moreover, in both RBC-V and RBC-P specimens, more viable cells were observed on the RBCs photo-cured with T2W when compared to RBCs photo-cured with TW. The lowest number of cells were observed when RBC-P was photocured with the single peak TW LCU.

When the surface-treated RBC specimens and the specimens containing the matrix components only with no filler were investigated for cell attachment (Supp. Fig. 4), the surface treatment (removal of surface layer) of RBC-V did not substantially influence cell attachment. In contrast, surface treatment on RBC-P improvement the cell attachment (Supp. Fig. 4a). The matrix only specimens of RBC-V showed good cell attachment whereas no cell attachment was observed on the matrix only specimens of RBC-P (Supp. Fig. 4b).

The influence of the different REs and the respective DCs upon cell numbers (both spread and round cells) on RBC spec-

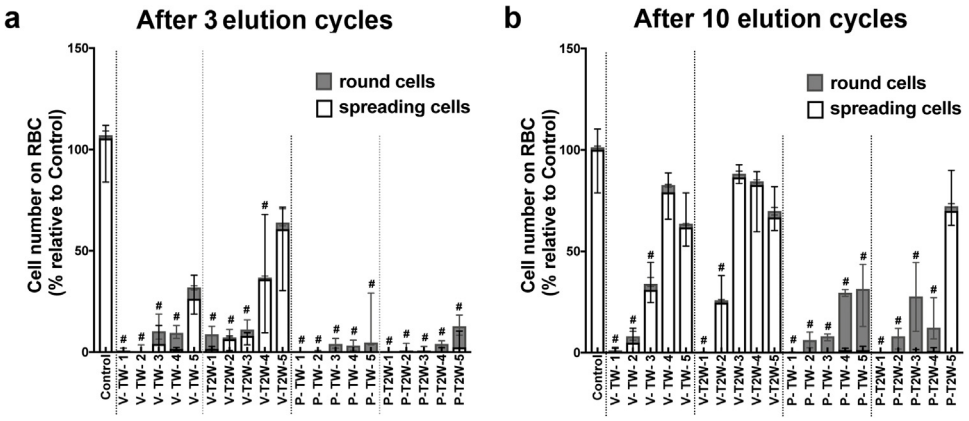

Fig. 6 – Relative cell attachment on RBCs at 24 h after 3 elution cycles and 24 h after 10 elution cycles. Both the numbers of round cells and spreading cells were calculated. (100% = optimal density reading of control cultures. #; significantly lower than the plastic control samples, $p < 0.05$. n = 9 medians with 25/75 percentiles).

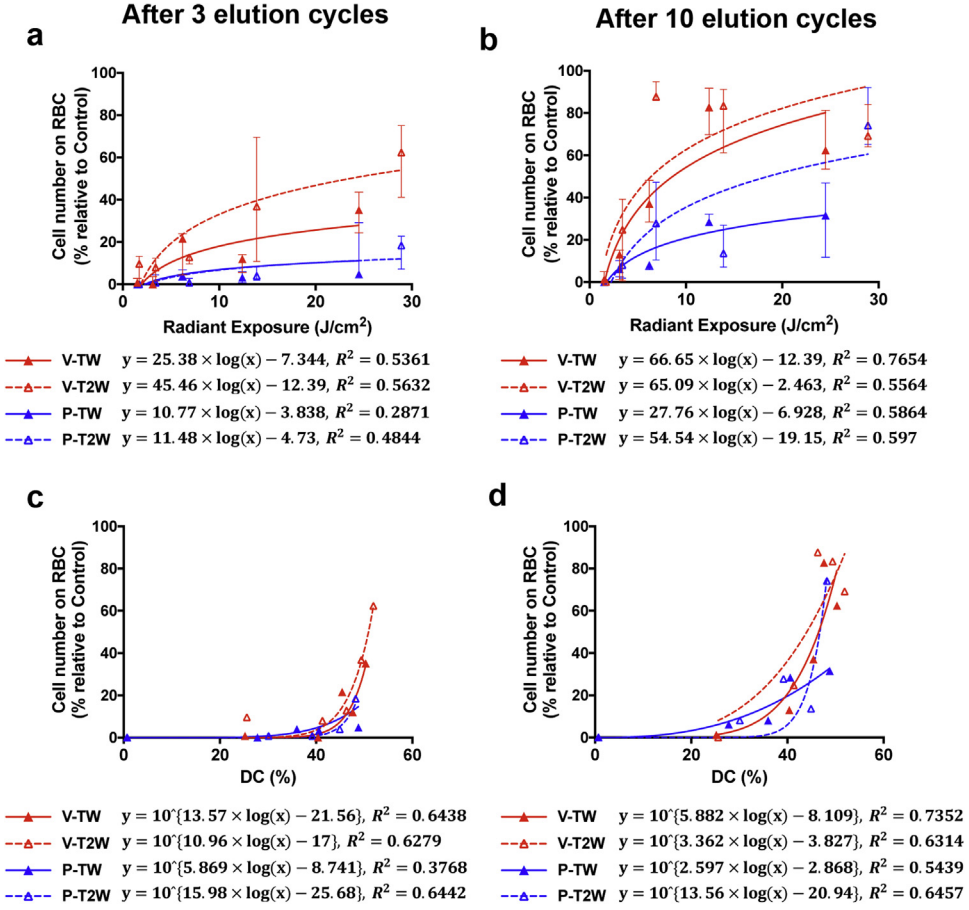

Fig. 7 – Influence of (a, b) radiant exposure and (c, d) DC on cell attachment (relative total cell number including both round and spreading cells) on composites after (a, c) 3 and (b, d) elution cycles at 24 h. The graphs represent (a, b) the medians with error bars 25/75 percentiles and fitting curves (semi-log line; x is slog, y is linear, least squares fit), and (c, d) median and fitting curves (log-log line; least squares fit) of the 9 specimens' values. (100% = optimal density reading of cultures on the plastic control).

imens is depicted in Fig. 7. Again, the above mentioned lower number of cells on RBC-P compared to RBC-V become apparent when plotting the cell numbers vs. the different REs (Fig. 7a and b) especially for the 3rd elution. Furthermore, more cells were counted on T2W cured specimens compared to those cured with TW. The combination of RBC-V with TW yielded low cell numbers even at the highest RE. The curve fitting resulted in a logarithmic equation for both specimens after

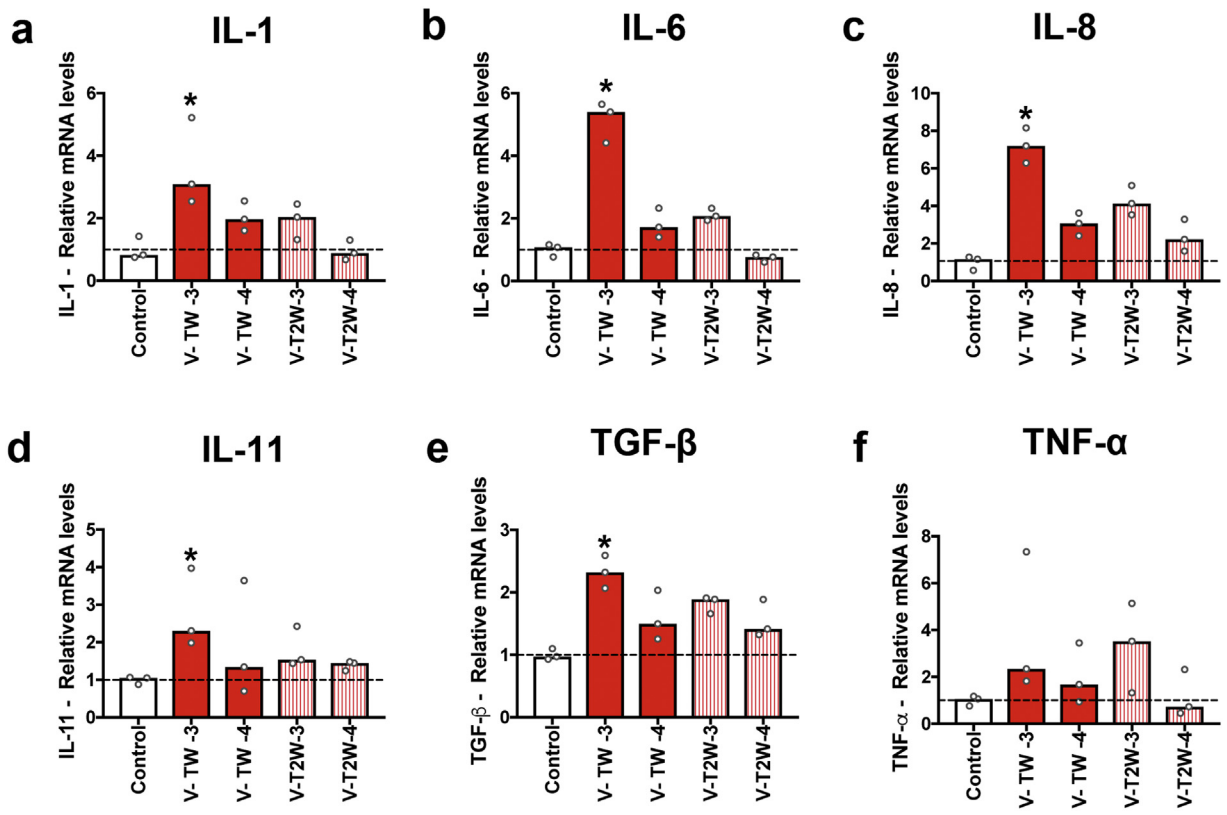

Fig. 8 – Results from real-time PCR of HGFs seeded on RBCs at 3 days for genes encoding (a) IL-1, (b) IL-6, (c) IL-8, (d) IL-11, (e) TGF-β, (f) TNF-α. (* denotes significantly higher than the plastic control, $p < 0.05$, n = 3, medians with min and max values represented by °).

3rd and 10th elution cycles. A plateau was reached for RBC-V at about 15–20 J/cm^2 for the 10th elution time point. For the 3rd elution, no plateau was observed.

Interestingly, plotting the cell numbers vs. the DC (Fig. 7c and d), the above-seen differences (Fig. 7a and b) were not or they were less apparent. For both, the 3rd and the 10th elution time point a logarithmic relation between cell numbers and DC can be observed. At a DC of around 50%, the cell number tended to reach its maximum at the 10th elution period (except for RBC-P with TW). This can be considered to be the DC which should be reached for optimal cell growth on the respective specimens. However, this value was not reached at the 3rd elution period.

3.5. *Gene expression of cells grown on RBCs*

Based on the results of cell growth potentials on RBCs, gene expression and protein release from HGFs cultured for 3 days were recorded for RBC-V cured with both LCUs at two different REs (20 s 25% of maximum exposure and 20 s 50% of maximum exposure) (Figs. 8 and 9). Respective tests with RBC-P could not be performed due to the low cell numbers on this material. The mRNA levels of IL-1, -6, -8, -11, TGF-β, integrin β3, caspase-9, annexin A5, and ADM on V-TW-3 specimens were significantly upregulated when compared to control on the tissue culture plastic. Interestingly, better photo-curing (20 s, 50% of maximum exposure) generally decreased mRNA levels of inflammatory cytokines (IL-1, IL-6, IL-8, and IL-11) on RBC-V specimens (Fig. 8). Also, specimens cured with T2W in most cases – and especially with IL-6 – evoked a smaller increase of the gene expression than specimens cured with TW. Furthermore, mRNA levels of ki-67 (a marker for cell proliferation) were significantly downregulated on the less cured specimens when compared to control tissue culture plastic, especially for the combination of RBC-V and TW. Better photo-curing increased mRNA levels of the proliferation marker (ki-67) on RBC-V specimens cured by the TW LCU (Fig. 9). Also, mRNA of apoptose markers (caspase 9, annexin A5) were upregulated at low REs, especially for RBC-V. The expression of apoptose markers Caspase 3 and 8 were upregulated, but not statistically significant. Parallel to this, the gene expression for ADM (adrenomedullin), a marker for increasing cell tolerance to oxidative stress, was significantly upregulated when a low RE was delivered to RBC-V. Similarly, the IL-6 released from cells seeded on RBC-V was significantly upregulated when compared to control tissue culture plastic (Fig. 10). Of note, better photo-curing tended to decrease the release of IL-6 from cells.

In summary, the results of gene expression of HGF on RBC specimens demonstrated that the lower DC/RE and using the TW rather than T2W LCU up-regulated inflammation markers level and apoptosis markers level and decreased the proliferation marker, ki-67. Similarly, the results of protein synthesis

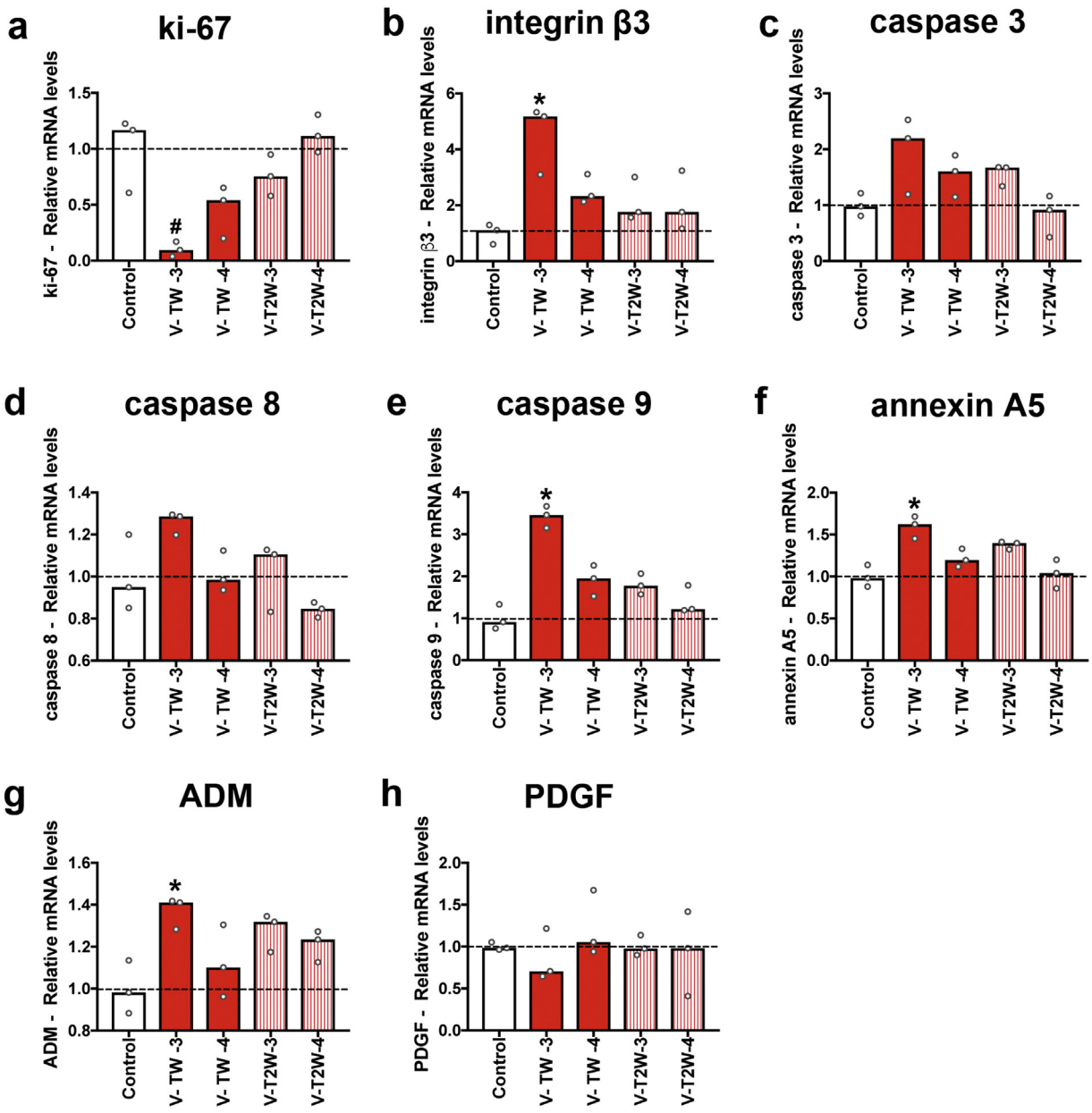

Fig. 9 – Results from real-time PCR of HGFs seeded on RBCs after 3 Elution cycles at 3 days for genes encoding (a) ki-67, (b) integrin β3, (c) caspase 3, (d) caspase 8, (e) caspase 9, (f) annexin A5, (g) ADM, (h) PDGF. (* denotes significantly higher than the plastic control, $p < 0.05$, # denotes significantly lower than the plastic control, $p < 0.05$, $n = 3$, medians with min and max values represented by °).

of HGF on RBC showed that at lower DC/REs using the TW LCU tended to increase the inflammation markers level.

3.6. *Cell viability after eluate exposure*

Cytotoxicity of RBC eluates collected at 4 different time points (1st, 2nd, 3rd, and 10th eluate) of the 20 groups after 24 h incubation/exposure are shown in Fig. 11. In general, the eluates collected at the later time points demonstrated less cytotoxicity for both, RBC-V and RBC-P, as well as for both LCUs. The eluates of the 10th elution did not negatively affect cell viability when compared to the control medium anymore. Thus, differences between the groups became more apparent at low numbers of elution cycles. Furthermore, the groups receiving less RE showed significantly lower cell viability in the 1st, 2nd, and 3rd eluates. In detail, eluates from RBC-V of the 1st, 2nd and 3rd eluates) (with few exceptions) evoked lower cell viability when compared RBC-P (Fig. 11a–c). For the first eluate, the combination of RBC-P and the TW LCU resulted in lower cell viability than using the same material with T2W.

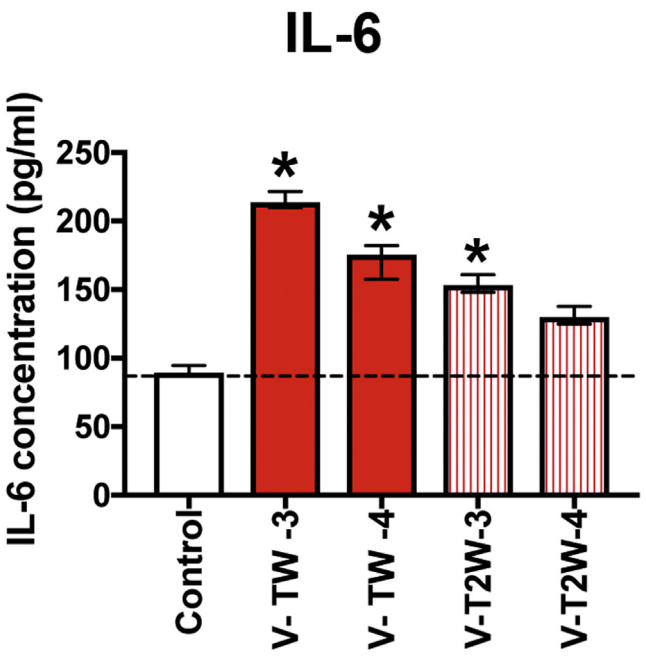

Fig. 10 – Protein release from HGFs seeded on composites after 3 elution cycles at 3 days of IL-6. (* denotes significantly higher than control plastic, $p < 0.05$, $p < 0.05$, $n = 6$, medians with 25/75 percentiles).

The influence of the different REs and the respective DCs on eluate cell viability for the 1st and the 3rd eluate is shown in Fig. 12. For the 10th eluate, no such influence was apparent from data presented in Fig. 11. The plots of cell viability vs. REs (Fig. 11a–c) show a logarithmic shape with an initially steep increase of cell viability with increasing RE, and a plateau is reached between 5 and 10 J/cm^2. Furthermore, the first and second eluates from RBC-V cured with both LCUs evoked mainly less cell viability than the eluates from RBC-P, e.g., for RE of >3.4 J/cm^2 from T2W LCU when cultured in the first eluate.

Comparison of the effect of the two LCUs revealed lower cell viability of the RBC specimens photocured with TW compared to the T2W LCU when testing the first eluate. For the first and the second eluate, the combination of RBC-V with TW yielded the lowest cell viability.

The influence of the different DCs upon cell viability (Fig. 12d–e) also shows a logarithmic curve shape for RBC-P for all eluates. For RBC-V, which generally showed lower cell viability at the same DCs as RBC-P, the data point for low DCs could not be reached (despite low RE) due to the experimental setup. Again, a logarithmic shape of the curves is apparent. Here, the same basic characteristics as described above (Fig. 12a–c) can be observed, here even at the 3rd eluate.

For the 1st elution, 100% cell viability indicating the DC, which does not produce eluate cytotoxicity, was only found for RBC-P together with T2W at a DC of around 40% (Fig. 12d–f). For the 2nd elution, it was around 30% for RBC-P and 50% for RBC-

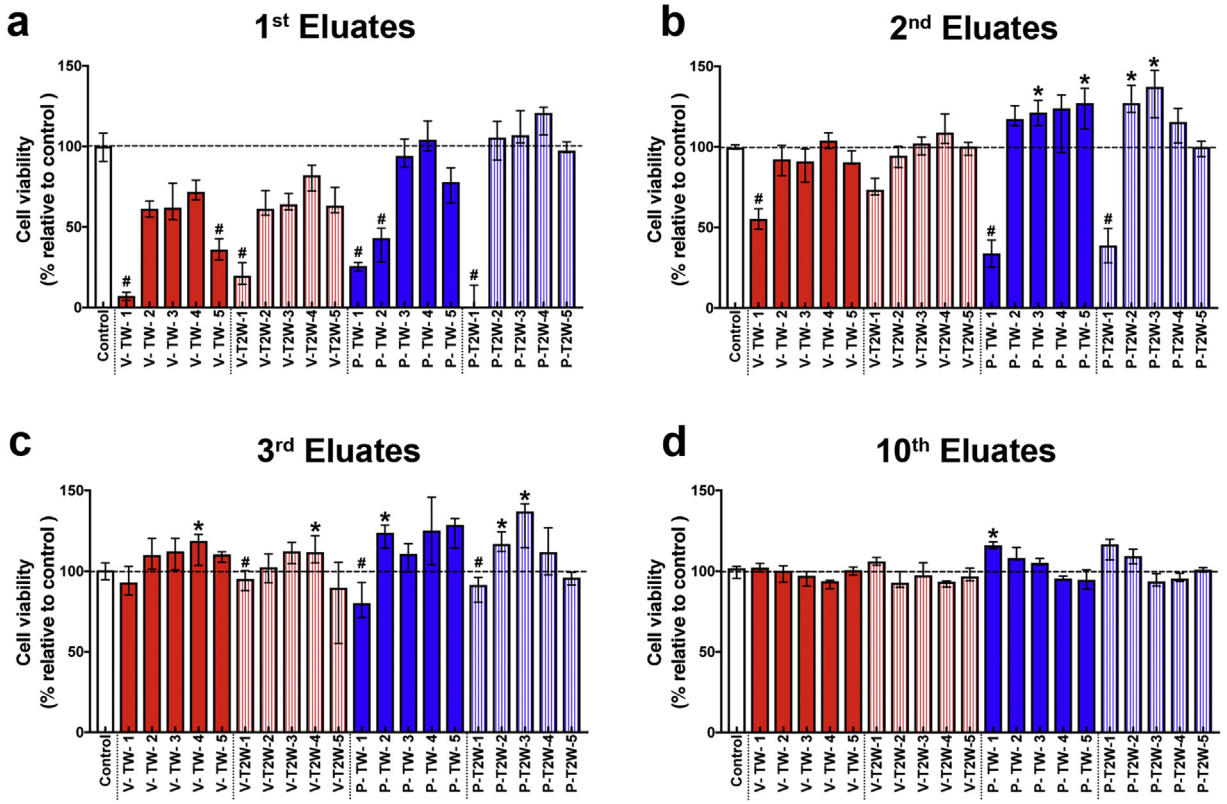

Fig. 11 – Relative cell viability of HGFs stimulated in eluates of composite materials at 24 h in (a) 1st eluates, (b) 2nd eluates, (c) 3rd eluates, and (d) 10th eluates. (* denotes significantly higher than control plastic, $p < 0.05$, # denotes significantly lower than the plastic control, $p < 0.05$, $n = 9$, medians with 25/75 percentiles).

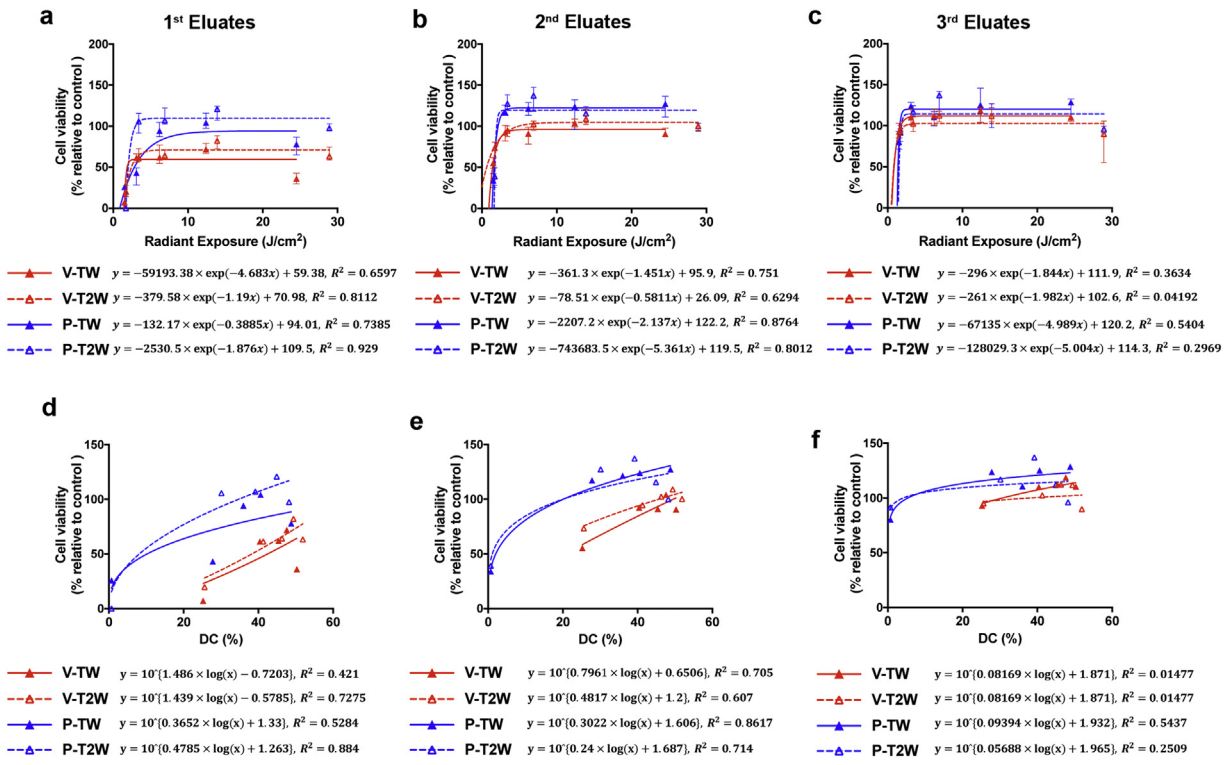

Fig. 12 – Influence of (a–c) radiant exposure and (d–f) DC on cell viability in (a, d) 1st eluates, (b, e) 2nd eluates, (c, f) 3rd eluates at 24 h. The graphs represent (a–c) the medians with error bars 25/75 percentiles and fitting curves (one-phase association line, least squares fit), and (d–f) median and fitting line (log-log line; least squares fit) of the 9 specimens' values. (100% = cell viability in control media).

V. For the 3rd elution the differences between the materials further decreased (Fig. 12d–f).

3.7. *Gene expression of cells after eluate exposure*

Lastly, the gene expressions and protein release from HGFs exposed to 3rd RBC eluates were investigated after 3 days incubation/exposure (Figs. 13–15). The mRNA levels of inflammation mediators IL-1, -8, and TNF-α from the least cured RBC-V, and RBC-P specimens by TW, (but not by T2W) were significantly upregulated when compared with control tissue culture material (Fig. 13a–c, f). The expression of mRNA for the inflammation mediator Il-6 was significantly upregulated for the RBC-P in combination with TW, for RBC-V with TW upregulation was not statistically significant. For IL-11, a tendency of upregulation of mRNA after exposure to eluates from the least cured RBC-V specimen with TW could be observed, but this was not statistically significant (Fig. 13d).

However, mRNA levels of PDGF (Fig. 14h) were significantly downregulated under the least well-cured conditions in RBC-P specimens cured with either LCUs when compared to control medium. In most specimens receiving higher RE, a decrease in mRNA expressions of inflammatory cytokines especially in groups treated with TW was observed. Nevertheless, no significant differences were found in any groups in apoptotic gene levels, including caspase 3, 8, 9 and annexin A5 (Fig. 14c–f).

Protein release patterns for measured cell markers from cells cultured in eluates were not consistent with mRNA levels of those cells (Fig. 15). Especially in RBC-P groups, using a low RE significantly decreased released protein levels of IL-6, TGF-β, and VEGF (Fig. 15a–d). Interestingly, eluates from RBC-V especially at low REs increased the expression of Il-6, and the influence of the RE upon the biological reaction can be seen. IL-1, TNF-α, PDGF-BB release was not detected by ELISA (data not shown).

In summary, the results of gene expression of HGF in eluates demonstrated that at the lower REs and DC, using the TW LCU rather than T2W up-regulated inflammation and apoptosis markers levels and decreased the expression of mRNA of the proliferation marker, ki-67. Both RBC-V and RBC-P showed similar inflammation marker expression pattern, whereas RBC-P, especially the combination of RBC-P and TW showed higher ki-67, a proliferation marker when compared to the RBC-V. The results of protein synthesis of HGF in eluates showed that at the lower REs and DC using RBC-P rather than RBC-V increased the inflammation and the angiogenesis marker levels.

4. Discussion

The present study aimed to investigate the influence of a range of radiant exposures and respective degrees of conver-

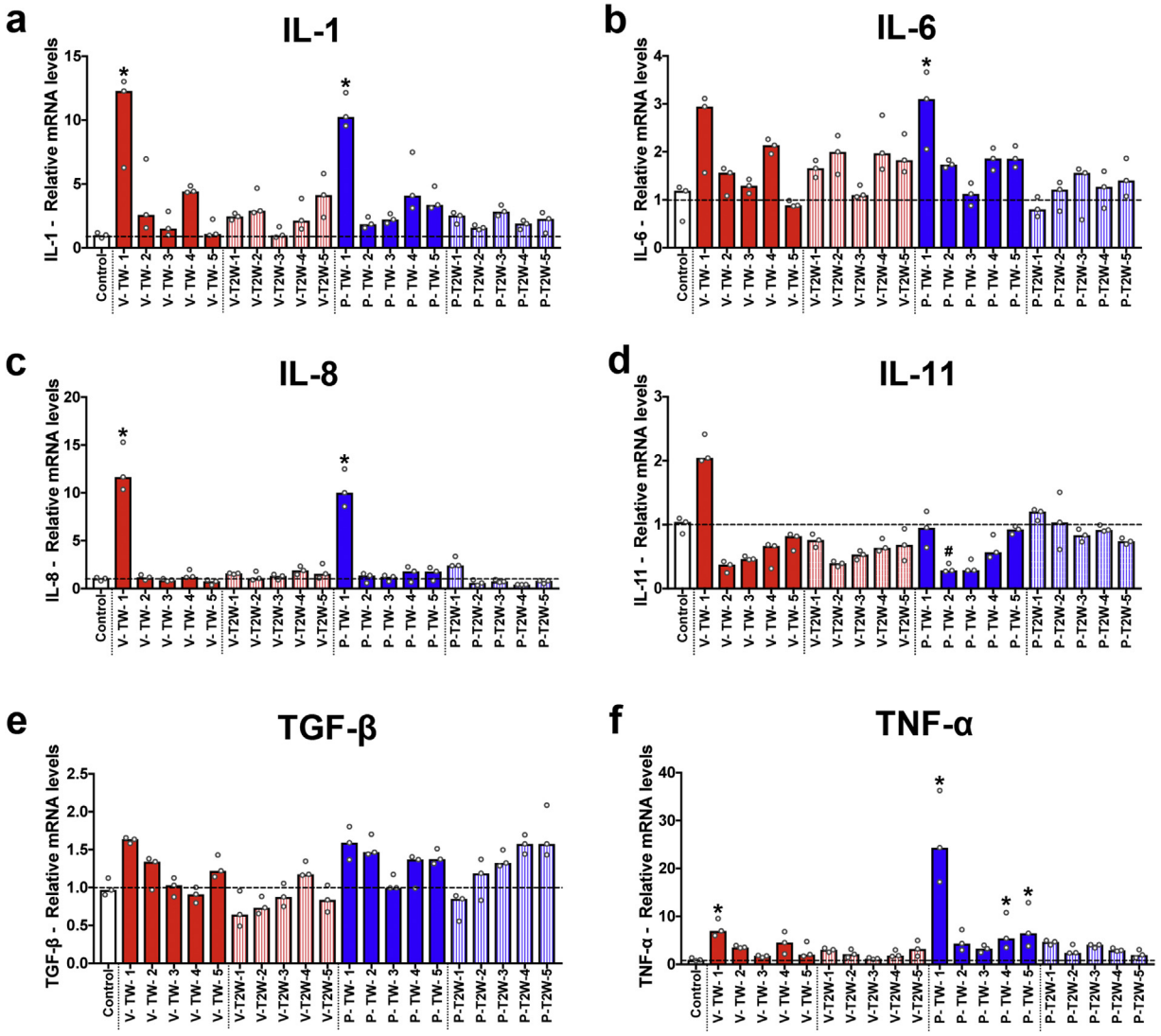

Fig. 13 – Results of real-time PCR of HGFs stimulated in composite eluates at 3 days for genes encoding (a) IL-1, (b) IL-6, (c) IL-8, (d) IL-11, (e) TGF-β, (f) TNF-α (* denotes significantly higher than the plastic control, # denotes significantly lower than the plastic control, $p < 0.05$, $n = 3$, medians with min and max values represented by °).

sion of two commercially available RBCs upon the reaction of gingival fibroblasts (HGFs), which were in direct contact with the test materials or exposed to material eluates. Tests were performed under different experimental conditions using RBCs with different compositions and two different LED-based LCUs, one emitting light above 420 nm (mono wave LCU), the other emitting an additional violet peak (a dual emission peak LCU). The intent was to deliver similar amounts of blue (>420 nm) energy to the RBCs so that the potential benefits of the violet light present could be determined. Finally, the influence of elution on material cytotoxicity was evaluated simulating a more prolonged exposure.

Particular emphasis in this study was placed on testing strictly characterized RBC specimens with defined surfaces in different cell culture systems and using different end-points. The RBCs were specifically chosen because, according to the information from the manufacturer, they differ in the chemical composition of the polymer matrix, one being Bis-GMA- based (RBC-V), the second being based on UDMA (RBC-P) (Table 1). Furthermore, both materials differed in the initiator systems. According to the information from the manufacturer, the conventional initiator system of RBC-V is based on CQ/Amine, whereas RBC-P is based on CQ with a blend of violet sensitive co-initiators. The inhibitor is the same in both materials. The LCUs were from the same manufacturer and were selected according to the different initiator systems used in two RBCs of this study, where especially RBC-P was intended to be cured with a dual emission peak LCU that delivers violet light as well as blue light.

HGFs were used as target cells as it is well recognized that the primary cells to contact RBCs clinically are gingival epithe-

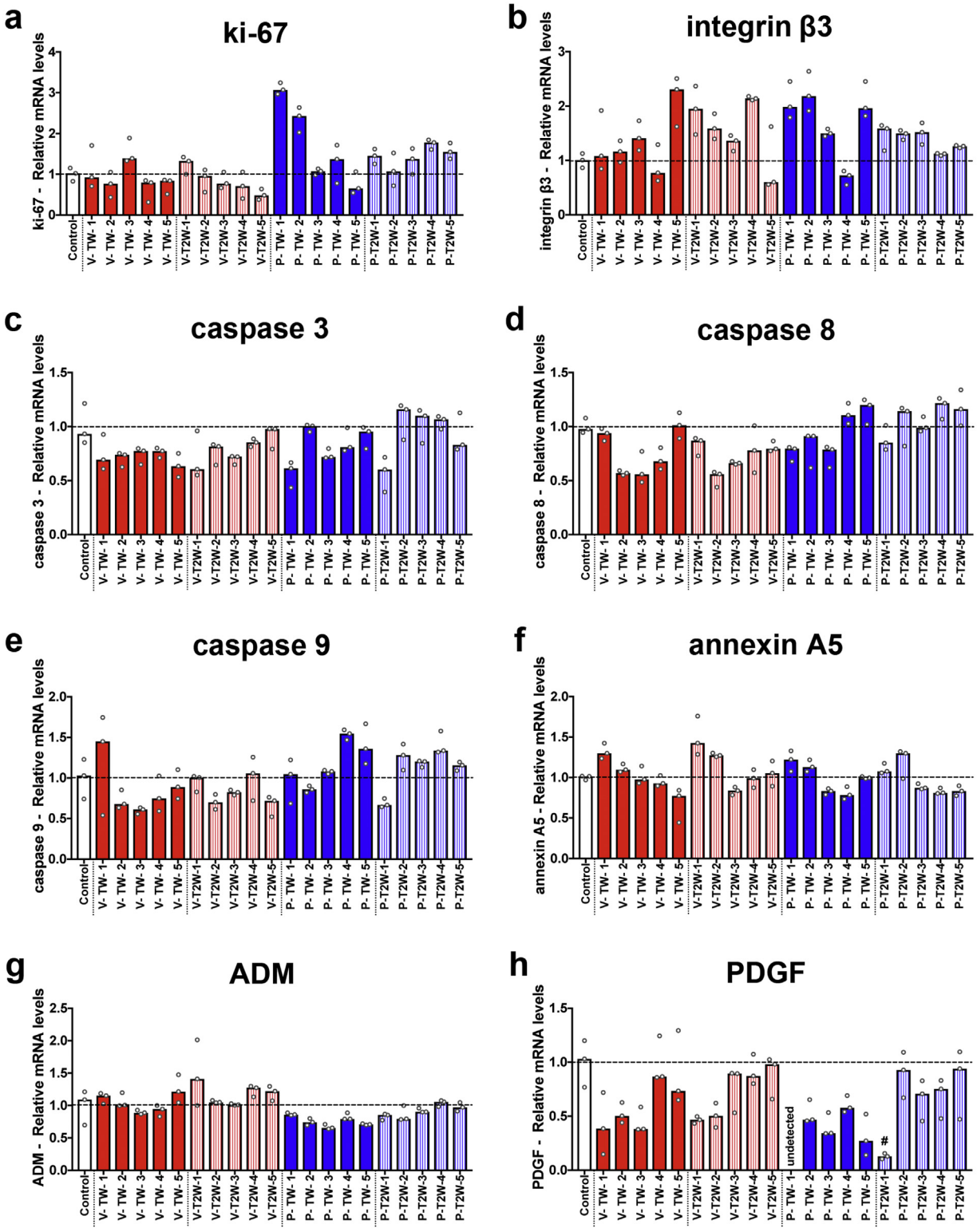

Fig. 14 – Results of real-time PCR of HGFs stimulated in 3rd composite eluates at 3 days for genes encoding (a) ki-67, (b) integrin β3, (c) caspase 3, (d) caspase 8, (e) caspase 9, (f) annexin A5, (g) ADM, (h) PDGF. (# denotes significantly lower than the plastic control, $p < 0.05$, $n = 3$, medians with min and max values represented by °).

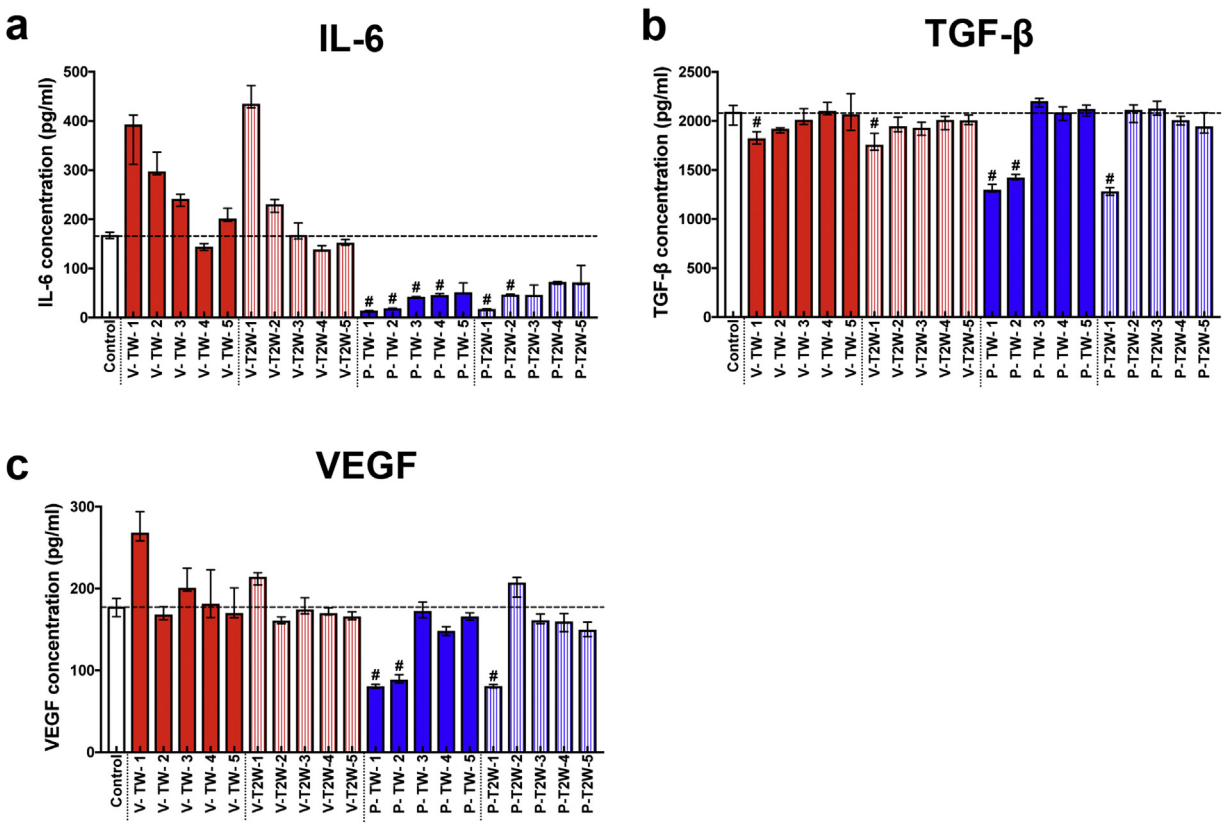

Fig. 15 – Protein release from HGFs seeded in 3rd composites eluates at 3 days of (a) IL-6, (b) TGF-β, (c) VEGF. (# denotes significantly lower than the plastic control, $p < 0.05$, $n = 6$, medians with 25/75 percentiles).

lial cells [31]. When preparing deep cavities reaching into the gingival sulcus, the gingival epithelium is inevitably touched and potentially removed. Thus, the newly placed RBC may also contact gingival fibroblasts, which also play an essential role in the resulting healing process. Furthermore, HGFs show better growth kinetics and ease of use compared to human gingival epithelial cells.

Cell viability assays with eluates were performed according to ISO standards (ISO 10993-5 and 10993-12) as previously reported [21], to complement the experiments for cell adhesion. In order to provide more mechanistic background information, gene expression of HGFs was recorded for relevant genetic markers for inflammation IL-1, IL-6, IL-8, IL-11, and TNF-α), apoptosis (caspase 3, caspase 8, caspase 9, annexin A5) or regenerative processes (ki-67, integrin β3, ADM, PDGF and TGF-β). To the best of our knowledge, such combined experiments with well-defined test specimens have not been done previously.

4.1. *Radiant exposures and resulting DC*

The REs delivered to the specimens ranged from 1.5 J/cm^2 to 28.9 J/cm^2 and were selected based on clinical considerations for different distances from the tip of the light guide to the material (0–12 mm) and different exposure times (5–20 s). We found a logarithmic relationship between REs and DC and a generally higher DC at the same REs for RBC-V compared to RBC-P. These results are in agreement with other reports. A higher DC of a Bis-GMA-based RBC compared to a urethane based RBC at the same REs was also found in a recent study, where RBC specimens had been exposed to either 5 or 10 J/cm^2 [32] where it was also reported that the DC of a Bis-GMA-based RBC was lower after 5 J/cm^2 than after 10 J/cm^2 RE. A logarithmic relationship between DC and exposure time was also reported by Cardoso et al. [6]. Another study directly measured the DC of RBCs after REs ranging from 3 to 48 J/cm^2, which comes close to the range of the present study [33]. Again, a logarithmic relationship was found between the DC and RE. In the present study, the presence of the violet peak in the T2W LCU resulted in a small, but statistically significant, increase in DC even when similar REs were delivered. The most likely explanation is that the CQ initiator is activated by blue light from the dual emission peak LCU, and the addition of Lucirin TPO initiator that has an optimal absorbance at around 385 nm and phenyl-propanedione that has an optimal absorbance at around 398 nm, to RBC-P, but not in RBC-V, improved the polymerization. Since the TW LCU delivered no light in the lower violet wavelength, this LCU produced the lowest DCs (Table 5). This observation reinforces the need to match the emission spectrum from the LCU with the absorption spectrum of the photoinitiators within the RBC. In the study mentioned above a plateau for DC was observed after delivering a RE of 20–25 J/cm^2, which is in the range of in the present results being around 15 J/cm^2 for RBC-V and 25 J/cm^2

for RBC-P cured with the single (blue light) emission peak LCU [33].

4.2. Degree of conversion and cell reactions

In the present study, virtually all the observed cell reactions were dependent upon the degree of conversion (DC) that, in turn, was dependent upon the RE, the material composition and the compatibility between the photoinitiators and the emission spectrum from the LCU. It is known from the literature that the higher the DC of tested RBCs, the lower is the amount of substances that are released [13,24,34] and this explains the observation that lower DC values result in less cell attachment and higher eluate cytotoxicity. Of note, we were able to parallel the differences in DC for each material with data from the biological experiments. For instance, the urethane-based RBC-P showed a lower DC compared to the Bis-GMA based RBC-V and thus lower cell numbers on RBC-P were observed than on RBC-V. Especially the combination of the RBC containing two initiator systems (RBC-P) with the LCU, which only referred to one initiator (camphorquinone) showed consistently lower DC on the one side and lower cell attachment, higher eluate cytotoxicity or higher expression of inflammation or apoptosis markers on the other side. This demonstrates that the biological system very sensitively reacts towards differences in DC, at least shortly after photocuring. Interestingly, no such relationship could be observed between the lower DC of RBC-P and the eluate cytotoxicity, which proved to be lower than RBC-V. This indicates that a more detailed and quantitative analysis of the relationship between DC and the cellular response should be conducted.

4.3. Elution cycles

In the present study, increasing the number of elution cycles lead to more cell attachment and less eluate cytotoxicity. This corroborates the results from previous studies that reported decreased elution of substances with increasing elution time [35] or with repeated elutions [12,36]. Also, after several elutions, the material surfaces may be covered with a protein layer from the cell culture medium, which also may favor cell attachment [37]. Repeated elution cycles might affect DC. However, in a recent study, most of the post-curing was found only up to 15 h after light exposure [38]. In the present study, the DC measurement was performed at 180 s after the LCU was turned on and likely would have increased during storage due to the effects of post-curing. However, the elution cycles took place much longer than 15 h after light exposure. Thus, the effects of post-curing can be ruled out as a reason for the decreasing toxicity after multiple elution cycles. Furthermore, the leachable components within the RBCs will decrease after each elution. However, during the early phase of the material application, healing processes, e.g. of damaged pulpal or gingival tissues may take place, and this timeframe is reflected in the results from tests using the eluates from the first few elution cycles (see below).

4.4. Materials composition

Cell attachment was reduced when in direct contact with RBC-P in comparison to RBC-V (Figs. 6 and 7, and Supp, Figs. 2 and 3). This difference cannot be explained by differences in wettability between the two RBCs, because contact angle measurements showed no differences between both RBCs (Fig. 4). The change of wettability after incubation with cell culture medium containing serum is likely due to the formation of a proteinous coating [39]. Also, eluate cytotoxicity cannot explain this difference, because opposing results were found (see also below).

However, the composition of the resin matrix in the RBC materials was different. Specimens, where the surface layer had been removed, showed a substantially increased cell attachment for RBC-P, whereas for RBC-V it stayed at the same high level (Supp. Fig. 4a). The surface layer of RBCs may potentially be more resin rich, and if this is removed by polishing, the cells are exposed to less resin and more filler particles [40]. Furthermore, specimens made by Kulzer GmbH that included just the polymer matrix did not show any cell attachment for RBC-P, but did show good attachment for RBC-V (Supp. Fig. 4b). From these results, it appears that the difference in cell attachment observed between the two RBCs from the same manufacturer (RBC-V and RBC-P) was due to their different chemical compositions.

Interestingly the difference in cell attachment between the two RBCs was not or less apparent when the cell numbers were plotted against the DC (Fig. 5). Therefore, it can be assumed that the different DC characteristics may also play a role in the differences in cell attachments behavior of the two RBCs. Furthermore, it has been reported that cell attachment and proliferation depend on surface chemistry and varies with individual functional groups rather than general surface properties such as wettability [20].

4.5. Biological endpoints

The difference mentioned above in cell attachment between the two RBCs was contrary to the results of the eluate cell viability tests, where RBC-P was less cytotoxic at corresponding REs and DCs especially for the 1st and 2nd eluate than RBC-V (Figs. 11 and 12). The cytotoxicity of eluates depends on the nature and the effective quantity/concentration of eluted substances, e.g., monomers [34,41,42]. In cultures of human gingival fibroblasts, a UDMA monomer (a component of RBC-P) proved to be less cytotoxic than a Bis-GMA monomer (a component of RBC-V) [34]. In the present study, the eluates were not further analyzed as this was beyond the scope of the study. However, this difference between the two monomers may be a reason for the lower cytotoxicity of RBC-P eluate compared to RBC-V. On the other hand, this reason cannot explain the difference in cell reaction in direct contact with the test materials, which was the opposite compared to the elution test. It can be speculated that either differences in surface chemistry (see above) or local concentration effects are responsible for this reaction. Time-dependent concentrations of substances released directly onto contacting cells may be different from a situation, where substances first are release into cell culture medium over some time (e.g., 24 h) and then exposed to

cells due to dilution or possible interactions with the culture medium. This is in line with the results of this study showing a more sensitive gene expression pattern for cell attachment assays than for elution tests.

Despite the difference between the two materials, both, cell attachment assay and the eluate assay demonstrated higher cell toxicity on the specimens with fewer elution cycles, and lower DC again showing the interrelation of the factors. For biological characterization of a restorative material, however, both the direct contact situation with relevant target cells and standard elution tests should be considered because the results may differ between these two test methods and the direct cell situation better reflects the local oral conditions in the gingival sulcus or the tooth pulp.

4.6. *Mechanistic aspects*

Inflammation markers: The mRNA levels of tested inflammatory markers IL-1, IL-6, IL-8, and TNF-α reflected the cytotoxic potential in both culture systems (Fig. 8 and 11) and were upregulated along with increasing cytotoxicity especially on low DC specimens. On the protein level, IL-6 concentrations were elevated after direct exposure of cells to low DC RBC-V specimens. Generally, inflammation marker upregulation depended upon the RE and the DC.

Upregulation of IL-6 and IL-8 has also been observed, when 3-D-cultures of reconstituted human epithelial cells (cancer cell line) had been exposed to non-toxic concentrations of TEGDMA, which is a commonly used acrylic monomer in RBCs [43]. In a further study a UDMA based endodontic sealer caused in pulp cells, PDL-cells and osteoblasts a significant upregulation of inflammation markers IL-6, IL-8, IL-12 and TNF-α parallel to a decrease in cell numbers. Also, upregulation of IL-6 after exposure of human gingival fibroblasts to extracts from chemically cured dental polymethacrylate materials has been reported [44,45].

In clinical studies, gingival sulcus fluid had been collected after the placement of subgingival Class V or II restorations using different materials [46,47]. With all materials concentrations of IL-6, IL-8 and TNF-α were higher than in control teeth with no materials. However, this increase may be due to several reasons, for example, plaque accumulation. Upregulation of inflammation mediators in the early phase of exposure to material in the gingival sulcus may interfere with the initial healing process. Inflammation usually causes slower healing [48]. Thus, increasing the inflammatory response during the early healing phase might have an adverse effect on wound healing [48].

Ki-67: In the present study mRNA expression of Ki-67 in cells with direct contact to the test materials with low DC was decreased. This is in line with data from immunostaining with Ki-67 antigens of mouse fibroblasts, were also reduced expression of Ki-67 after exposure to more than 10 mM Bis-GMA was observed [49]. Schweikl et al. reported that the acrylic monomer TEGDMA caused cell cycle delays through p53-dependent and independent pathways in the various cell lines [50]. This indicates a reduction of cell proliferation and can be seen in the context of the above-mentioned increase of inflammation markers [48]. Thus, the initial healing potential of gingival tissues in contact with RBCs that have a low DC may be inhibited.

TGF-β was significantly increased when cells were in direct contact with RBC that had a low DC. TGF-β has many functions in the oral environment; e.g., stimulating tertiary dentin formation [51]. It is also involved in wound healing: in experimental animals, TGF-β signal transduction blockage increased healing [52,53]. However, it also plays a role in keeping the ROS-balance of the cells by increasing the uptake of cystine leading to better maintenance of cellular glutathione during oxidative stress [54]. RBC monomers such as TEGDMA and HEMA have been shown to cause a ROS imbalance [55,56] and the upregulation of TGF-β can be regarded as an adaptive cell mechanism.

Integrin and ADM: Integrin binding specificity regulates biomaterial surface chemistry effects on cell differentiation [57]. In the present study, the groups that were most cured (specifically the V-TW-5, P-TW-5) demonstrated over a 2-fold increase in gene expression supporting the favorable attachment of gingival fibroblasts towards highly cured resin composites. Adrenomedullin (ADM) has also previously been shown to increase fibroblast-like synoviocyte adhesion to extracellular matrix proteins by upregulating integrin activation [58]. In the present study, no differences in gene expression of ADM were observed between all groups. It may, therefore, be assumed that ADM does not play a role in gingival fibroblast attachment to RBCs.

Apoptosis markers (caspase 9, and annexin A5) were significantly upregulated in direct cell material contact assays as well as (not significantly) caspases 3 and 8. This further confirmed the relevance to more cytotoxic behavior, whereas these gene expressions were not affected in an elution culture system. The resin monomer substances induced apoptosis in several cell types through the generation of redox balance-disturbing reactive oxygen species (ROS), which results in DNA damage, followed by cell apoptosis [5,42,59].

Interestingly, the combination of RBC-P and TW displayed comparatively high mRNA expressions at the lowest radiant exposure for IL-6 and TNF-α and a significant decrease of PDGF mRNA expression (growth factor for cell migration, proliferation, and angiogenesis). Other genetic markers revealed some interesting tendencies such as the upregulation of Ki-67, caspase 9 and the downregulation of PDGF, but these were not significantly different from controls.

4.7. *Clinical relevance*

The radiant exposure and the DC of RBCs influence their biological behavior in a dose-dependent manner that is mainly a logarithmic function. Consequently, in low RE situations, even a small difference in the RE can cause a large difference in the cell reaction. Conversely, little effect is observed at higher REs. Biological effects are more pronounced in situations where there is direct cell contact to the RBC than when the effect of the eluates is examined. Cell deaths, as well as induction of inflammation, apoptosis and reduced cell proliferation, are expected to occur after material placement. This local effect may interfere with the tissue healing if the gingival tissues have been traumatized during the tooth preparation or when filling the cavity.

Thus, it is reasonable to establish a critical minimum RE that the RBC should receive based on the DC, biological reactions or mechanical properties. Based on the DC, it appears that the minimum RE should be between 15 to 25 J/cm^2 for the two RBCs tested. For cellular reactions, the situation is more complicated, because these data depend not only on DC but also on a number of modifying parameters. Based on data from cell attachment tests (Fig. 7) 100% cell attachment does not occur after 3 elution cycles, even at a high DC, but does occur after 10 elution cycles, at which point this DC causes almost no cell reaction. Thus, to prevent adverse local effects it is suggested that a radiant exposure of more than 25 J/cm^2 is advisable.

Photo-curing a 2 mm thick RBC that includes photoactivators that require violet light (RBC-P) using an LCU that emits only blue light yielded inferior results, both for DC and in the biological tests. Therefore, it is advisable that the emission profile of the LCU should include the wavelengths of light that cover the absorbance profile of the initiators used in the RBC.

5. Conclusions

Cell attachment/viability of human gingival fibroblasts in contact with the RBCs or their eluates generally depended on the degree of conversion, the material composition and the number of eluate cycles (elution time). Cell reactions were more pronounced in direct contact with test specimens than when eluates were tested, and thus the local healing processes of the gingival tissues may be impaired by insufficient curing. The RBC matrix components of RBC-V showed greater cell attachment when compared to RBC-P, and eluates from RBC-V demonstrated lower cell viability when compared to RBC-P. Furthermore, the dual emission peak LCU that delivered violet as well as blue light, especially for the acute effects (low number of elutions), resulted in better cell attachment and less eluate cytotoxicity due to the presence of the additional violet light. It was concluded that the inclusion of the violet light from the T2W was beneficial, and the combination of the dual emission peak T2W LCU, RBC-V, exposure delivering more than 25 J/cm^2 reached the greatest DC that also had the least cell response.

Acknowledgements

This work is supported in part by Kulzer GmbH, Hanau, Germany.

Appendix A. Supplementary data

Supplementary material related to this article can be found, in the online version, at doi:https://doi.org/10.1016/j.dental.2019.05.015.

REFERENCES

[1] Gaengler P, Hoyer I, Montag R. Clinical evaluation of posterior composite restorations: the 10-year report. J Adhes Dent 2001;3:184–94.
[2] Brunthaler A, König F, Lucas T, Sperr W, Schedle A. Longevity of direct resin composite restorations in posterior teeth: a review. Clin Oral Investig 2003;7:63–70.
[3] Federation FWD. FDI policy statement on dental amalgam and the Minamata Convention on Mercury: adopted by the FDI General Assembly: 13 September 2014, New Delhi, India. Int Dent J 2014;64:295–6.
[4] Harlow J, Rueggeberg F, Labrie D, Sullivan B, Price R. Transmission of violet and blue light through conventional (layered) and bulk cured resin-based composites. J Dent 2016;53:44–50.
[5] Schmalz G, Arenholt-Bindslev D. Biocompatibility of dental materials. Springer; 2009.
[6] Cardoso KA, Zarpellon DC, Madruga CF, Rodrigues JA, Arrais CA. Effects of radiant exposure values using second and third generation light curing units on the degree of conversion of a lucirin-based resin composite. J Appl Oral Sci 2017;25:140–6.
[7] Geurtsen W. Substances released from dental resin composites and glass ionomer cements. Eur J Oral Sci 1998;106:687–95.
[8] Inoue K, Hayashi I. Residual monomer (Bis-GMA) of composite resins. J Oral Rehabil 1982;9:493–7.
[9] Spahl W, Budzikiewicz H, Geurtsen W. Determination of leachable components from four commercial dental composites by gas and liquid chromatography/mass spectrometry. J Dent 1998;26:137–45.
[10] Van Landuyt K, Nawrot T, Geebelen B, De Munck J, Snauwaert J, Yoshihara K, et al. How much do resin-based dental materials release? A meta-analytical approach. Dent Mater 2011;27:723–47.
[11] Ferracane J. Elution of leachable components from composites. J Oral Rehabil 1994;21:441–52.
[12] Sevkusic M, Schuster L, Rothmund L, Dettinger K, Maier M, Hickel R, et al. The elution and breakdown behavior of constituents from various light-cured composites. Dent Mater 2014;30:619–31.
[13] Högg C, Maier M, Dettinger-Maier K, He X, Rothmund L, Kehe K, et al. Effect of various light curing times on the elution of composite components. Clin Oral Investig 2016;20:2113–21.
[14] Pearson G, Longman C. Water sorption and solubility of resin-based materials following inadequate polymerization by a visible-light curing system. J Oral Rehabil 1989;16:57–61.
[15] Sigusch BW, Pflaum T, Völpel A, Schinkel M, Jandt KD. The influence of various light curing units on the cytotoxicity of dental adhesives. Dent Mater 2009;25:1446–52.
[16] Sigusch BW, Volpel A, Braun I, Uhl A, Jandt KD. Influence of different light curing units on the cytotoxicity of various dental composites. Dent Mater 2007;23:1342–8.
[17] Wegehaupt FJ, Lunghi N, Belibasakis GN, Attin T. Influence of light-curing distance on degree of conversion and cytotoxicity of etch-and-rinse and self-etch adhesives. BMC Oral Health 2016;17:12.
[18] Michaud PL, Price RB, Labrie D, Rueggeberg FA, Sullivan B. Localised irradiance distribution found in dental light curing units. J Dent 2014;42:129–39.

[19] Anselme K. Osteoblast adhesion on biomaterials. Biomaterials 2000;21:667–81.
[20] Schweikl H, Müller R, Englert C, Hiller K-A, Kujat R, Nerlich M, et al. Proliferation of osteoblasts and fibroblasts on model surfaces of varying roughness and surface chemistry. J Mater Sci Mater Med 2007;18:1895–905.
[21] Schweikl H, Hiller K-A, Bolay C, Kreissl M, Kreismann W, Nusser A, et al. Cytotoxic and mutagenic effects of dental composite materials. Biomaterials 2005;26:1713–9.
[22] Setzer B, Bächle M, Metzger MC, Kohal RJ. The gene-expression and phenotypic response of hFOB 1.19 osteoblasts to surface-modified titanium and zirconia. Biomaterials 2009;30:979–90.
[23] Zreiqat H, Howlett CR. Titanium substrata composition influences osteoblastic phenotype: in vitro study. J Biomed Mater Res A 1999;47:360–6.
[24] Schulz SD, Rüppell C, Tomakidi P, Steinberg T, Reichl F-X, Hellwig E, et al. Gene expression analysis of conventional and interactive human gingival cell systems exposed to dental composites. Dent Mater 2015;31:1321–34.
[25] Urcan E, Scherthan H, Styllou M, Haertel U, Hickel R, Reichl F-X. Induction of DNA double-strand breaks in primary gingival fibroblasts by exposure to dental resin composites. Biomaterials 2010;31:2010–4.
[26] Tadin A, Marovic D, Galic N, Kovacic I, Zeljezic D. Composite-induced toxicity in human gingival and pulp fibroblast cells. Acta Odontol Scand 2014;72:304–11.
[27] Styllou M, Reichl F-X, Styllou P, Urcan E, Rothmund L, Hickel R, et al. Dental composite components induce DNA-damage and altered nuclear morphology in gingiva fibroblasts. Dent Mater 2015;31:1335–44.
[28] Schweikl H, Hiller KA, Bolay C, Kreissl M, Kreismann W, Nusser A, et al. Cytotoxic and mutagenic effects of dental composite materials. Biomaterials 2005;26:1713–9.
[29] Wang Y, Zhang Y, Jing D, Shuang Y, Miron RJ. Enamel matrix derivative improves gingival fibroblast cell behavior cultured on titanium surfaces. Clin Oral Investig 2016;20:685–95.
[30] Kobayashi E, Fujioka-Kobayashi M, Sculean A, Chappuis V, Buser D, Schaller B, et al. Effects of platelet rich plasma (PRP) on human gingival fibroblast, osteoblast and periodontal ligament cell behavior. BMC Oral Health 2017;17:91.
[31] Moharamzadeh K, Van Noort R, Brook IM, Scutt AM. Cytotoxicity of resin monomers on human gingival fibroblasts and HaCaT keratinocytes. Dent Mater 2007;23:40–4.
[32] Cuevas-Suarez CE, Pimentel-Garcia B, Rivera-Gonzaga A, Alvarez-Gayosso C, Ancona-Meza AL, Grazioli G, et al. Examining the Effect of Radiant Exposure on Commercial Photopolimerizable Dental Resin Composites. Dent J (Basel) 2018;6:55.
[33] Calheiros FC, Daronch M, Rueggeberg FA, Braga RR. Degree of conversion and mechanical properties of a BisGMA:TEGDMA composite as a function of the applied radiant exposure. J Biomed Mater Res B Appl Biomater 2008;84:503–9.
[34] Reichl F-X, Esters M, Simon S, Seiss M, Kehe K, Kleinsasser N, et al. Cell death effects of resin-based dental material compounds and mercurials in human gingival fibroblasts. Arch Toxicol 2006;80:370–7.
[35] Ferracane J, Marker V. Solvent degradation and reduced fracture toughness in aged composites. J Dent Res 1992;71:13–9.
[36] Rothmund L, Shehata M, Van Landuyt KL, Schweikl H, Carell T, Geurtsen W, et al. Release and protein binding of components from resin based composites in native saliva and other extraction media. Dent Mater 2015;31:496–504.
[37] Schweikl H, Hiller K-A, Carl U, Schweiger R, Eidt A, Ruhl S, et al. Salivary protein adsorption and Streptococccus gordonii adhesion to dental material surfaces. Dent Mater 2013;29:1080–9.
[38] Germscheid W, de Gorre LG, Sullivan B, O'Neill C, Price RB, Labrie D. Post-curing in dental resin-based composites. Dent Mater 2018;34:1367–77.
[39] Müller R, Ruhl S, Hiller KA, Schmalz G, Schweikl H. Adhesion of eukaryotic cells and Staphylococcus aureus to silicon model surfaces. J Biomed Mater Res A 2008;84:817–27.
[40] Janus J, Fauxpoint G, Arntz Y, Pelletier H, Etienne O. Surface roughness and morphology of three nanocomposites after two different polishing treatments by a multitechnique approach. Dent Mater 2010;26:416–25.
[41] Urcan E, Haertel U, Styllou M, Hickel R, Scherthan H, Reichl FX. Real-time xCELLigence impedance analysis of the cytotoxicity of dental composite components on human gingival fibroblasts. Dent Mater 2010;26:51–8.
[42] Goldberg M. In vitro and in vivo studies on the toxicity of dental resin components: a review. Clin Oral Investig 2008;12:1–8.
[43] Schmalz G, Schweikl H, Hiller KA. Release of prostaglandin E2, IL-6 and IL-8 from human oral epithelial culturemodels after exposure to compounds of dental materials. Eur J Oral Sci 2000;108:442–8.
[44] Diomede F, Caputi S, Merciaro I, Frisone S, D'arcangelo C, Piattelli A, et al. Pro-inflammatory cytokine release and cell growth inhibition in primary human oral cells after exposure to endodontic sealer. Int Endod J 2014;47:864–72.
[45] Borelli B, Zarone F, Rivieccio V, Riccitiello F, Simeone M, Sorrentino R, et al. Polyacrylic resins regulate transcriptional control of interleukin-6, gp80, and gp130 genes in human gingival fibroblasts. J Oral Sci 2017;59:87–91.
[46] Ilday NO, Celik N, Dilsiz A, Alp HH, Aydin T, Seven N, et al. The effects of silorane composites on levels of cytokines and periodontal parameters. Contemp Clin Dent 2013;4:437–42.
[47] Celik N, Askin S, Gul MA, Seven N. The effect of restorative materials on cytokines in gingival crevicular fluid. Arch Oral Biol 2017;84:139–44.
[48] Martin P, Leibovich SJ. Inflammatory cells during wound repair: the good, the bad and the ugly. Trends Cell Biol 2005;15:599–607.
[49] Sarafian V, Uzunova Y, Hayrabedyan S, Ganchevska P, Filipova M, Filipov I, et al. Histo-blood group antigen expression and proliferative activity of fibroblasts treated with dental monomers. Cell Biol Toxicol 2008;24:27–37.
[50] Schweikl H, Altmannberger I, Hanser N, Hiller K-A, Bolay C, Brockhoff G, et al. The effect of triethylene glycol dimethacrylate on the cell cycle of mammalian cells. Biomaterials 2005;26:4111–8.
[51] Schmalz G, Widbiller M, Galler KM. Signaling molecules and pulp regeneration. J Endod 2017;43:S7–11.
[52] Ashcroft GS, Yang X, Glick AB, Weinstein M, Letterio JJ, Mizel DE, et al. Mice lacking Smad3 show accelerated wound healing and an impaired local inflammatory response. Nat Cell Biol 1999;1:260–6.
[53] Jinno K, Takahashi T, Tsuchida K, Tanaka E, Moriyama K. Acceleration of palatal wound healing in Smad3-deficient mice. J Dent Res 2009;88:757–61.
[54] Pauly K, Fritz K, Furey A, Lobner D. Insulin-like growth factor 1 and transforming growth factor-β stimulate cystine/glutamate exchange activity in dental pulp cells. J Endod 2011;37:943–7.
[55] Eckhardt A, Gerstmayr N, Hiller K-A, Bolay C, Waha C, Spagnuolo G, et al. TEGDMA-induced oxidative DNA damage and activation of ATM and MAP kinases. Biomaterials 2009;30:2006–14.

[56] Schweikl H, Spagnuolo G, Schmalz G. Genetic and cellular toxicology of dental resin monomers. J Dent Res 2006;85:870–7.
[57] Keselowsky BG, Collard DM, García AJ. Integrin binding specificity regulates biomaterial surface chemistry effects on cell differentiation. Proc Natl Acad Sci 2005;102:5953–7.
[58] M-DA Kioon, Asensio C, Ea H-K, Uzan B, Cohen-Solal M, Lioté F. Adrenomedullin increases fibroblast-like synoviocyte adhesion to extracellular matrix proteins by upregulating integrin activation. Arthritis Res Ther 2010;12:R190.
[59] Krifka S, Hiller K-A, Spagnuolo G, Jewett A, Schmalz G, Schweikl H. The influence of glutathione on redox regulation by antioxidant proteins and apoptosis in macrophages exposed to 2-hydroxyethyl methacrylate (HEMA). Biomaterials 2012;33:5177–86.